



Cite this: *Chem. Soc. Rev.*, 2024, **53**, 8182

Received 29th April 2024

DOI: 10.1039/d4cs00409d

rsc.li/chem-soc-rev

Ion transport mechanisms in covalent organic frameworks: implications for technology

Wonmi Lee, ^a Haochen Li, ^a Zhilin Du^b and Dawei Feng ^{*ab}

Covalent organic frameworks (COFs) have emerged as promising materials for ion conduction due to their highly tunable structures and excellent electrochemical stability. This review paper explores the mechanisms of ion conduction in COFs, focusing on how these materials facilitate ion transport across their ordered structures, which is crucial for applications such as solid electrolytes in batteries and fuel cells. We discuss the design strategies employed to enhance ion conductivity, including pore size optimization, functionalization with ionic groups, and the incorporation of solvent molecules and salts. Additionally, we examine the various applications of ion-conductive COFs, particularly in energy storage and conversion technologies, highlighting recent advancements and future directions in this field. This review paper aims to provide a comprehensive overview of the current state of research on ion-conductive COFs, offering insights into their potential to design highly ion-conductive COFs considering not only fundamental studies but also practical perspectives for advanced electrochemical devices.

1. Introduction

Covalent organic frameworks (COFs) have been developed since they were firstly discovered by Yaghi and co-workers in 2005 due to their advantageous features for various applications.¹ COFs are a class of porous crystalline materials composed of

light elements such as carbon, hydrogen, oxygen, and nitrogen. The organic units are connected by covalent bonds to form reticular frameworks with periodic channel structures. The unique and advantageous features of COFs are their lightweight, crystallinity, superior thermal and electrochemical stability, and porosity (Scheme 1).^{2–6} In particular, the main strength is the easy tunability of COF structures. This tunability can create structural diversity, and it can lead to tuning the properties of COFs in the desired direction depending on the applications we want to apply.^{7,8} Therefore, there are a lot of applications using COFs: gas storage, catalysis, sensing, energy

^a Department of Materials Science and Engineering, University of Wisconsin – Madison, Madison, Wisconsin 53706, USA. E-mail: dfeng23@wisc.edu

^b Department of Chemistry, University of Wisconsin – Madison, Madison, Wisconsin 53706, USA



Wonmi Lee

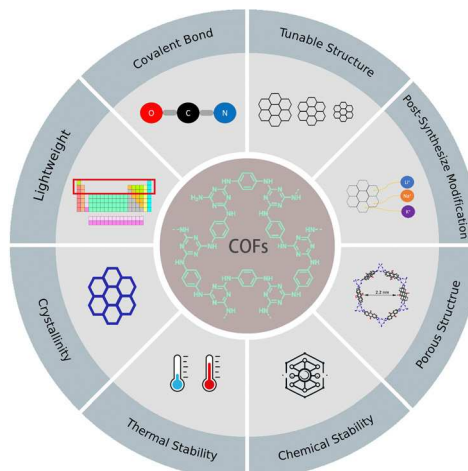
Wonmi Lee received her bachelor's degree in Chemical and Biomolecular Engineering from Seoul National University of Science and Technology in 2017. Afterwards, she completed her MSc and PhD in New Energy Engineering under the supervision of Prof. Yongchai Kwon at the same institution, in 2019 and 2022, respectively. Currently, she is a research associate in Materials Science and Engineering in Prof. Dawei Feng's group at the University of Wisconsin-Madison. Her research is focused on covalent organic frameworks and their potential applications in energy storage and conversion applications.



Haochen Li

Haochen Li obtained his bachelor's degree in Power Engineering from North China University of Science and Technology in 2019. Afterwards, he completed his MSc in Thermal Power Engineering under the supervision of Prof. Songfeng Tian at North China Electric Power University in 2021. Currently, he is a PhD student in Materials Science and Engineering in Prof. Dawei Feng's group at the University of Wisconsin-Madison. His research

is focused on covalent organic frameworks and their potential applications in energy storage and conversion applications.



Scheme 1 Unique features of COFs.

storage and conversion areas like batteries and supercapacitors, and environmental applications such as water purification.^{9–14}

In this review, the ion-conducting properties of COFs will be mainly covered, considering their potential in applications such as battery electrolytes, fuel cells, and other energy storage and conversion devices. Ion transport is important to enhance the performance of electrochemical devices because the ion transport is much slower than electron transfer, which is a critical control step in the electrochemical reactions when using them as electrodes.¹⁵ In addition, the solid conductors are important to replace the conventionally used liquid electrolytes for more safe batteries, and the poor ion mobility was the main hurdle to prevent their practical application.^{16,17} In liquid electrolytes, solvent and solvated molecules quickly exchange in a uniform environment. On the other hand, in solid conductors, ions should navigate through periodic bottlenecks and

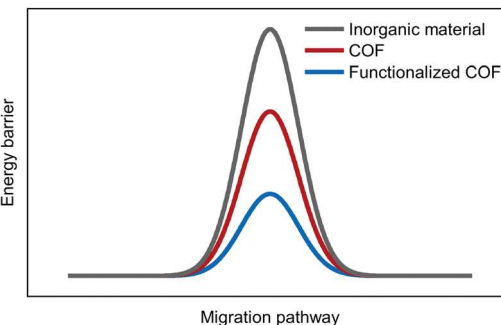


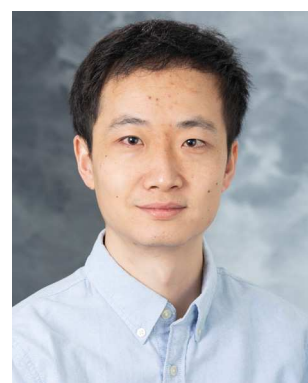
Fig. 1 Ion conduction scheme and energy barrier graph of inorganic material, COF, and functionalized COF.

overcome energy barriers to move.^{18,19} COFs are key alternatives to the conventionally used inorganic or polymeric materials because they exhibit superior ion conducting behavior due to their unique features such as well-defined directional channels, functional diversity, structural robustness, low ionic diffusion energy barrier, and excellent temperature tolerance.^{20,21} COFs have both advantageous features of high orderliness of inorganic materials and high tailorability of polymers and can eliminate the drawbacks of inorganic or polymer materials.²² In addition, when incorporating the ionic groups inside the structures of COFs, the functionalized COFs can further decrease the ion diffusion energy barrier (Fig. 1).^{23,24}



Zhilin Du

Zhilin Du is currently a bachelor's student in Chemistry and Computer Science in Prof. Dawei Feng's group at the University of Wisconsin-Madison. His research focuses on the synthesis, electrochemical, and theoretical computational characterization of covalent organic frameworks.



Dawei Feng

Dawei Feng received his bachelor's degree in Chemistry from Peking University in 2009. Afterwards, he completed a PhD in Chemistry under the supervision of Prof. Hong-Cai Zhou at Texas A&M University in 2015. After that, he was working as a postdoctoral researcher in Chemical Engineering in Prof. Zhenan Bao's group at Stanford University. Currently, he is an assistant professor in Materials Science and Engineering and Chemistry at the University of Wisconsin-Madison. He received a National Science Foundation CAREER Award. His research is focused on the development of novel metal-organic or covalent organic frameworks for electronic devices and as solid-state ion conductors for batteries.

The purpose of this review is emphasizing the uniqueness of COFs compared to inorganic or polymeric materials in terms of ion conducting properties by looking at ion diffusion mechanisms with different ion conduction pathways, activation energy, mobile ion concentration, and transference number. In addition, the rational design strategies of ion-conductive COFs through structural modification, incorporation of solvent and additional solvent, and processing optimization are provided. Finally, future studies such as mechanism understanding studies, considering cost and scalability for practical usage in various real devices, are discussed.

2. COF's uniqueness compared to inorganic and polymeric materials

2.1 Structural features

The structural diversity of COFs stems from the tunability in topology and chemistry by choosing an appropriate symmetry of building blocks and linkage chemistries. First, the topological tunability can be achieved by using a different geometry of building blocks. The dimensions and topology of COFs can be determined by how the building blocks are spatially arranged, which is directly influenced by the shape and connectivity of the building blocks (Fig. 2).²⁵ There are mainly two-dimensional (2D) and three-dimensional (3D) COFs, and 2D COFs will be mainly focused on in this review. 2D COFs exhibit unique properties that can make them more advantageous than 3D COFs regarding ion conductivity due to an increased accessible surface area, tunable interlayer spacing, flexibility in modification, and solution-processability.^{26,27} These benefits can make 2D COFs particularly suitable for applications in energy storage and conversion devices, where fast ion transport is crucial. Specifically, more exposed surface area can provide more ion conduction sites and accessible pores, thereby facilitating ion transport. The basic units of COFs are connected through covalent bonds to create planar, interconnected layers. These layers are subsequently stacked on top of each other, forming complex multi-layer frameworks that incorporate directional one-dimensional nanochannels, and the ion diffusion can also occur through this inter-layer pathway, leading to rapid ion conduction.

Furthermore, modification of the surface chemistry in 2D COFs is easy, allowing for the introduction of various ionic groups that can enhance the ion diffusion. There are various topologies of COFs such as tetragonal, hexagonal, rhombic, and trigonal, based on the symmetry of the monomers. Second, the chemical tunability of COFs can also be obtained by choosing the different organic building blocks. The common building blocks to form the covalent bonds are boronic acids, aldehydes, amides, or amines, and different types of linkages such as boroxine, imine, hydrazone, or triazine can be made.^{28–31} Even one monomer can make the covalent bonds by themselves, and two different monomers can also make various types of linkages (Fig. 3). In addition, the different number of reaction sites that can form the covalent bonds for various monomers

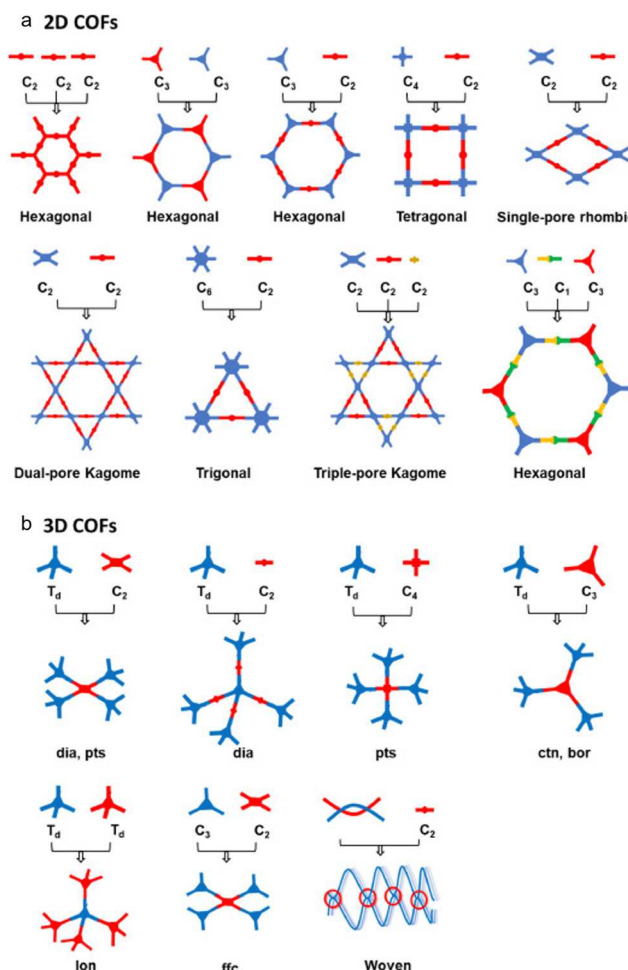


Fig. 2 Topological tunability of (a) 2D COFs and (b) 3D COFs (reproduced from ref. 25) with permission from Elsevier.

should also be considered to design an accurate molar ratio to synthesize the desired structures of COFs. Even though the COFs were synthesized with the same symmetries, the different structural and functional properties such as crystallinity or ionic conductivity would be achieved when using different chemistries of monomers. In addition, the different reversibility of different covalent linkages can result in different crystallinity, recyclability, and chemical stability. The reversible linkages of COFs typically enable high crystallinity due to the dynamic error correction during synthesis.³² This error correction allows the framework to reorganize during the formation, leading to more ordered structures. For example, imine (C=N) linkages are reversible under acidic conditions, which helps in the formation of highly crystalline structures.³³ In addition, the reversible covalent bonds can be beneficial for the recyclability of COFs. COFs can be disassembled into their building blocks and then reassembled easily, reducing waste, and enabling the reuse of materials.³⁴ However, the reversibility of linkages can lead to reduced stability under certain conditions.³⁵ Therefore, sometimes irreversible and robust linkages for highly stable COFs are developed. The COFs with these linkages exhibit

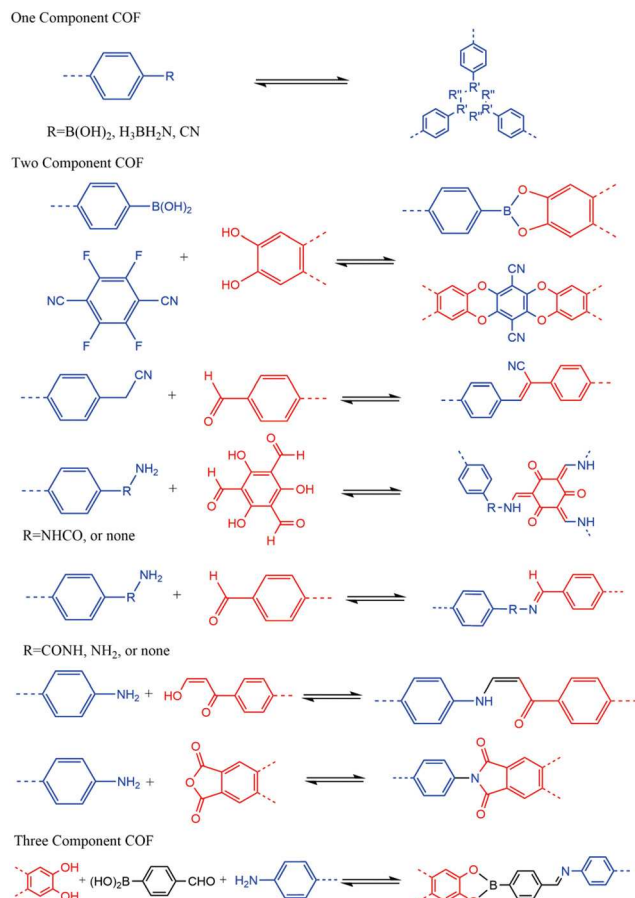


Fig. 3 Chemical tunability of COFs.

superior chemical stability in harsh environments. However, the robustness of these linkages generally makes COFs less recyclable. The trade-off relationship between crystallinity, recyclability and stability depending on the reversibility of

covalent linkages should be considered for designing COFs to meet the requirements of specific applications. Moreover, the all-organic nature makes COFs facile and flexible to the introduction of functional groups into their frameworks, which is beneficial for ion-conduction. The introduction of specific functional groups into COFs can tailor their interaction with ions, enhancing ion conductivity. Functional groups such as sulfonic acid, amine, and carboxylic groups can interact with ions through various mechanisms such as coordination, ion–dipole interactions, or by providing a pathway for hopping conduction.^{36–39} More detailed ion conducting mechanisms of functionalized COFs will be discussed later in section 3.1.

2.2 Ion diffusion mechanisms

The unique features of COFs, including their long-range ordered channels, high stability, low density, and their capability for functionalization, position them as promising candidates for solid electrolytes. In particular, COFs have shown potential for achieving high ionic conductivity. Unlike inorganic and polymer SEs, which often present a high energy barrier to the migration of bulky ions due to the segmental motion of polymers or the rigid crystalline spaces of inorganic solids, COFs can significantly lower the energy barrier for ion diffusion.^{40–42} This is attributed to their intrinsic open channels, offering ample void space for the rapid diffusion of various ions, regardless of size. This mechanism of ion conduction through COFs could potentially lead to superior ionic conductivities for bulky ions (Fig. 4).

More specifically, the ion migration in the inorganic solid materials mainly relies on the distribution and concentration of defects. Here, the defects can be divided into vacancies and interstitials.⁴³ The cationic vacancies or interstitials are considered as the mobile charge species. The ion diffusion mechanism in the inorganic solid materials can be considered as three pathways (Fig. 5a). First, vacancy diffusion occurs when

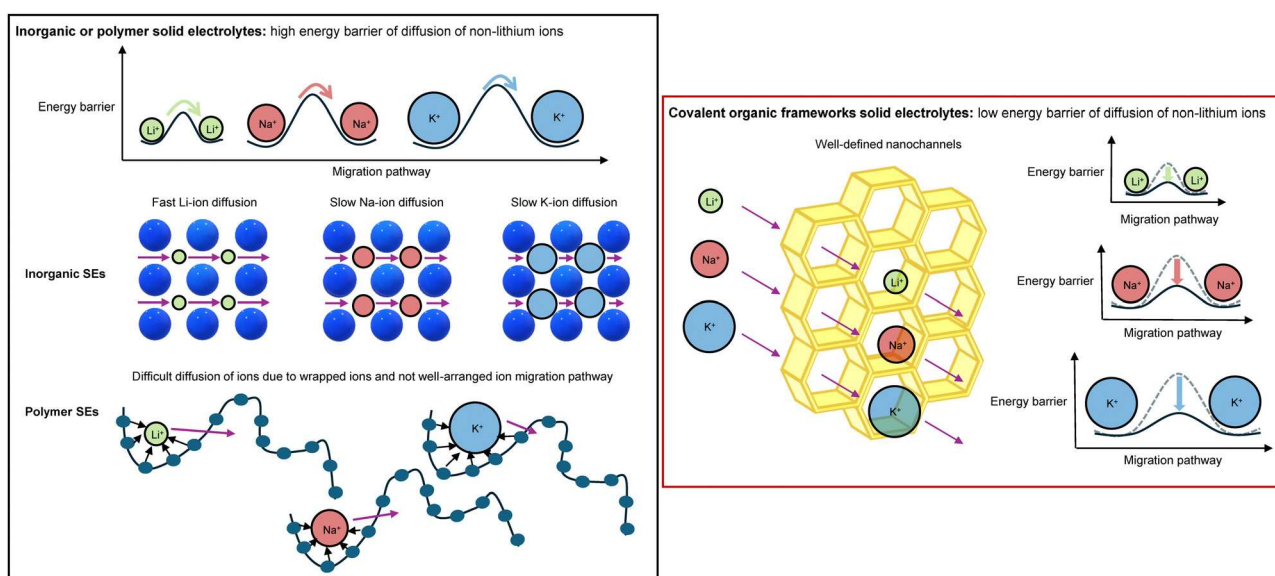


Fig. 4 Scheme for comparing the brief ion conduction mechanism in inorganic, polymers, and COFs.

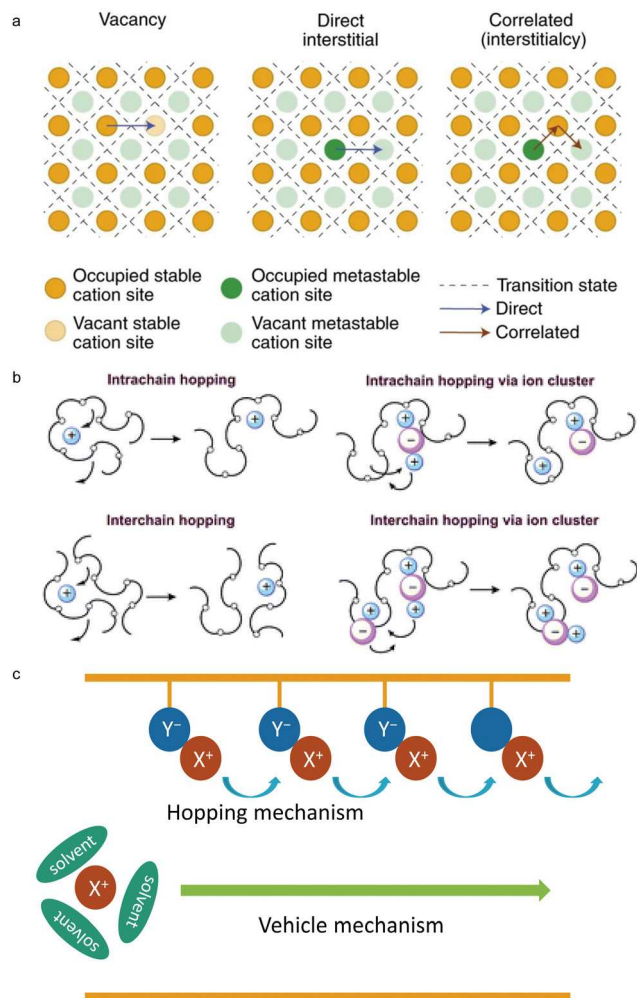


Fig. 5 Ion conduction mechanism of (a) inorganic materials (reproduced from ref. 43 with permission from Springer Nature), (b) polymer materials, (reproduced from ref. 50 with permission from the Royal Society of Chemistry) and (c) COFs.

an ion moves into an adjacent empty site. Second, a direct interstitial mechanism involves movement between partially occupied sites. Third, in the correlated interstitialcy process, migrating interstitial ions shift a nearby lattice ion to an adjacent position. Defects such as vacancies or interstitials can provide ion conducting pathways. Therefore, the higher defect concentrations can facilitate greater ion mobility, thereby increasing ion conductivity. However, the concentration of defects should be optimized because too many defects can lead to structural instability and other undesirable properties. The defect levels can be controlled by some strategies such as doping, sintering, chemical substitution, or annealing in controlled atmospheres.⁴⁴⁻⁴⁷ In addition, the valence and size of mobile ions greatly affect the ionic conduction.^{48,49} When the valence increases, the ionic conductivity decreases due to the strong electrostatic interaction between the mobile ions and solid skeleton. The impact of the size of mobile ions on ion conductivity is more complex than valence. When the size of the mobile ions is too large, the resistance of ion diffusion will

increase, then the diffusivity of mobile ions will decrease. On the other hand, when the size of the mobile ions is too small, they occupy sites with a large electrostatic trap, leading to difficulties in migrating. In the case of polymer materials, the ion conducting mechanism can be performed through intrachain or interchain hopping (Fig. 5b).⁵⁰ The mobile ions are coordinated with the polar groups in the polymer chain, and the free volumes are created for the hopping of mobile ions with the segmental motion of the chains. The intrachain hopping involves the movement of ions along a single polymer chain. This mechanism is facilitated by the flexibility of the polymer backbone and the presence of ionic or polar groups attached to the polymer chain that can temporarily bind ions.⁵¹ The process typically involves three steps. First, the ions bind to specific sites on the polymer chain, which are often ionic groups or other polar functionalities. Second, as the polymer chain undergoes segmental movements, the ion can move from one site to another along the chain. This movement might be assisted by the rotation of bonds within the polymer backbone or by the stretching and bending of the chain. Third, the ions are released from one site and can either rebind to a new site on the same chain or hop to another chain. This interchain hopping depends on the mobility of the polymer chain and the strength of interaction between the ion and the chain. On the other hand, the interchain hopping involves ions moving between different polymer chains. This hopping is crucial in more rigid or closely packed polymer systems where intrachain mobility is limited. It also involves three steps. First, ions dissociate from a binding site on one polymer chain. Second, the ions move to another polymer chain. This movement can occur through the polymer matrix or along interfaces where polymer chains meet. Third, the ion binds to a site on a neighboring polymer chain. This hopping can be influenced by the density and arrangement of the polymer chains, the spacing between them, and the dielectric constant of the medium. Interchain hopping is more common in polymers with high crystallinity or tight packing, where intrachain pathways are less accessible.⁵²

COFs exhibit a distinct ion transfer mechanism compared to many inorganic and polymer materials due to the unique properties of their ordered structures and high porosity, which can be precisely tuned at the molecular level.⁵³ The ordered 1D nanochannels of COFs can provide a fast ion-conduction pathway with a large free volume.⁵⁴ In addition, the customizable nanochannels by introducing ionic functional groups can facilitate the ion conductivity.⁵⁵ These groups can interact electrostatically or through hydrogen bonding with mobile ions, helping to solvate and mobilize them. The ion transport mechanisms in COFs can be classified into two types: the hopping mechanism and the vehicle mechanism (Fig. 5c). First, the hopping mechanism involves the movement of ions from one site to another site.⁵⁶ In COFs, this typically involves ions moving facilitated by electrostatic interactions or coordination with functional groups embedded in the framework. The hopping can be modulated by the framework's ability to coordinate with ions through functional groups which can act as binding

sites that temporarily capture and release the ions, thereby enabling their transport across the framework. Second, the vehicle mechanism describes ion transport that occurs along with a molecule that acts as a carrier.⁵⁷ This mechanism is relevant in systems where COFs are impregnated with a solvent (like water or an organic solvent) that can solvate the ions. The solvent molecules effectively “carry” the ions through the framework, with the solvent acting as a medium in which the ions are dissolved, aiding their diffusion through the material. The distance between the hopping sites will affect the ion conductivity. The shorter distance between the hopping sites can facilitate the ion transport. It can be modulated by regulating the stacking mode or introducing the ionic functional groups.⁵⁸ In addition, the solvent or salt can make different solvation environments, thereby affecting the ion diffusion.⁵⁹

2.3 Activation energy (energy barrier)

The activation energy for the ion conduction in the solid materials refers to the energy needed to enable the movement of ions through the solid materials, overcoming various types of energy barriers.⁶⁰

In inorganic solid conductors such as ceramic and glasses, their energy barriers are usually related to lattice structure, thermodynamic and kinetic barriers, and electrochemical stability.⁶¹ The crystal lattice of inorganic solids often provides a more rigid pathway for ion migration than in COFs. Ions move through the lattice by hopping from one stable site to another, influenced heavily by the presence of vacancies or interstitial sites.

Unlike inorganic materials, polymers can offer flexibility, which allows for expansion or contraction accommodating ionic pathways. This elasticity can reduce the mechanical energy barriers but may introduce others related to the arrangement of polymer chains. Ions in polymers typically migrate through amorphous rather than crystalline regions, where they encounter fewer barriers related to rigid lattice structures.⁶² However, they might still face significant resistance from viscous drag within the polymer matrix. In addition, polymer materials often require a certain temperature to maintain amorphous phases that are conducive to ion migration, which can limit their use in low-temperature applications.⁶³

On the other hand, the energy barriers in COFs for ion conduction can be considered with pore size, chemical compatibility and interaction, and structural stability. The pore size of COFs determines whether ions can physically pass through the COFs or not. When a pore size is too small, it physically blocks the ion, acting as a steric barrier. Therefore, to optimize the ion transport, the pore size can be tuned.⁶⁴ In addition, the functional groups within the pores of COFs can interact with ions, either facilitating or hindering their movement. These interactions might involve electrostatic forces, hydrogen bonding, or even π - π interactions, depending on the mobile ions and functional groups.⁶⁵ For example, COF with carboxylic groups might facilitate the transport of metal cations through ion-dipole interactions, enhancing conduction compared to a neutral pore surface. Moreover, the structural stability of COFs also might affect the energy barrier.⁶⁶

Overall, COFs can exhibit lower activation energy for ion conduction compared to inorganic or polymer materials due to their unique structural and chemical features. COFs are characterized by their highly ordered and tunable porous structures. This regularity can potentially facilitate more predictable pathways for ion migration compared to inorganic or polymer materials. The inorganic materials require ions to overcome higher energy barriers associated with defect sites, and the randomness of the polymer structure can create inconsistent pathways that increase the activation energy for ion transport.⁶⁷ On the other hand, the precise control over pore sizes and connectivity in COFs allows for the design of pathways that can minimize the energy required for ion conduction. In addition, chemical functionalization of pore walls in COFs can be tailored to interact favorably with specific ions, thereby reducing the activation energy for their transport. In contrast, modifying the internal surface chemistry of inorganic materials is more challenging, potentially leading to higher activation energies for ion movement. Moreover, COFs tend to be more flexible than many rigid inorganic materials. This flexibility can accommodate ions more readily, potentially reducing the strain and energy required for ion conduction through the transport pathways.⁶⁸ On the other hand, the rigidity of inorganic materials might necessitate higher energy to mobilize ions, especially when moving through tight lattice structures.

The activation energy for ion conduction can be determined experimentally using techniques like electrochemical impedance spectroscopy (EIS), which measures the frequency response of a material to an electrical stimulus.⁶⁹ From these measurements, the temperature dependence of the ionic conductivity can be obtained and used to calculate the activation energy *via* the Arrhenius equation:

$$\sigma T = \sigma_0 \exp\left(-\frac{E_a}{kT}\right)$$

here, σ is the conductivity at temperature T , σ_0 is a pre-exponential factor (related to the number of mobile ions and their attempt frequency), E_a is the activation energy, k is the Boltzmann constant, and T is the absolute temperature.

Understanding and minimizing the activation energy in solid electrolytes is crucial for improving the efficiency of devices such as batteries and fuel cells. Lower activation energies imply easier ion movement, which enhances the ionic conductivity and overall performance of the electrolyte at lower temperatures. This knowledge aids the design of better materials for energy storage and conversion technologies. Table 1 summarizes the activation energies of various types of solid conductors.^{70–133} Most COFs show high activation energies due to their structural benefits for ion conduction. Even though some of the other inorganic or polymer materials also exhibit high activation energies, they have some disadvantages. For example, many high-performance inorganic materials require high-temperature processing or complex synthesis routes that can be costly and energy-intensive.¹³⁴ COFs, on the other hand, are often synthesized at relatively low temperatures through

Table 1 Ion conducting properties summarized for inorganic, polymer, and COF materials

Type	Chemical formula	$\sigma_{(RT)}$ mS cm ⁻¹	E_a eV	Ion concentration ions cm ⁻³	Transference number	Ref.
Na-ion	NASICON $\text{Na}_{3.4}\text{Sc}_2\text{Si}_{0.4}\text{P}_{2.6}\text{O}_{12}$	6.9	0.33	3.99×10^{21}		70
	$\text{Na}_{3.3}\text{Zr}_{1.7}\text{Pr}_{0.3}\text{Si}_2\text{PO}_{12}$	6.7	0.235	3.46×10^{21}		73
	$\text{Na}_3\text{Zr}_2(\text{SiO}_4)_2\text{PO}_4$ (NZSP)	0.411	0.12	3.46×10^{21}		76
	β Alumia $\text{Na}\text{-}\beta''\text{-Al}_2\text{O}_3$ ($\text{Na}_2\text{O}\cdot 5.33\text{ Al}_2\text{O}_3$)	2.1	0.1	3.25×10^{21}		77
Sulfide	$\beta\text{-Al}_2\text{O}_3$	12	0.16			78
	Na_3SbS_4	1	0.24	5.66×10^{21}		80
	Na_3PS_4	1 ~ 2		6.99×10^{21}		81
Halide	NaTaCl_6	3.7	0.19	3.56×10^{21}	1	82
	Na-LaCeZrHfTa-Cl	4.62	0.3	3.79×10^{21}		87
	Na_4OI_2	4		3.61×10^{21}		88
Polymer	PEO + 10 wt% NaTFSI + 40 wt% BMIMTFSI	0.0162	0.68	9.13×10^{21}		
	PEO16-NaPF ₆	0.41	0.12		0.39	91
	PEO16-NaPF ₆ (50 °C)	0.63 (50 °C)			0.58	92
	PEO-NaBF ₄ -SN (36:1:8)	0.05	0.363			93
COF	PDPE-20	3.31	0.1			94
	NaOOC-COF + NaPF ₆ + PC	0.268	0.24		0.9	95
	TPDBD-CNa-QSSE + 9 wt% PC + 5 wt% FEC	0.13	0.204		0.9	96
	MIL-121/Na + 50 wt% NaClO ₄ + PC	0.1	0.36			97
	MOF-808-SO ₃ K + PC	0.031	0.32		0.76	98
	i-COF-1 (Na)	0.141	0.28	1.22×10^{21}		Manuscript submitted
	i-COF-2 (Na)	0.317	0.21	1.48×10^{21}		
K-ion	i-COF-3 (Na)	0.275	0.24	1.66×10^{21}		
	COF i-COF-1 (K)	0.137	0.21	1.22×10^{21}		Manuscript submitted
	i-COF-2 (K)	0.102	0.21	1.34×10^{21}		
Li-ion	i-COF-3 (K)	0.142	0.25	1.28×10^{21}		
	LISICONs $\text{Li}_{10}\text{Ge}(\text{P}_{0.975}\text{Sb}_{0.025})_2\text{S}_{12}$	16.6	0.26	2.1×10^{22}		99
	$\text{Li}_{10}\text{Ge}(\text{P}_{0.9}\text{Sb}_{0.1})_2\text{S}_{12}$	13.5	0.276	2.06×10^{22}		
	$\text{Li}_{3.2}\text{Ge}_{0.2}\text{P}_{0.8}\text{O}_4$	0.001	0.53	4.06×10^{22}		100
Halide	$\text{Li}_{3.5}\text{Ge}_{0.5}\text{V}_{0.5}\text{O}_4$	0.096	0.39	6.9×10^{22}		101
	$\text{Li}_{1.5}\text{Al}_{0.5}\text{Ge}_{1.5}(\text{PO}_4)_3$	0.75	0.725	7.38×10^{21}		103
	Li_3ErCl_6	0.31	0.41	1.38×10^{22}		104
Sulfides	$\text{Li}_3\text{YBr}_{5.7}\text{F}_{0.3}$	1.8	0.39	1.15×10^{22}		106
	$\text{Li}_{0.54}\text{Si}_{1.74}\text{P}_{1.44}\text{S}_{11.7}\text{Cl}_{0.3}$	25		1.98×10^{22}	1	108
	$\text{Li}_{10.25}\text{P}_3\text{S}_{12.25}\text{I}_{0.75}$	9.1	0.28	2.30×10^{22}		
Organic	$\text{Li}_{10.2}[\text{Sn}_{0.8}\text{Si}_{0.2}]_{1.2}\text{P}_{1.8}\text{S}_{12}$	2.5		2.09×10^{22}		111
	PEO-PS	0.095 (60 °C)	0.103		0.22	113
	SLIC-3 + 20% LiTFSI + 20% DEGDME + 2% SiO ₂	0.12	0.07			114
	PEO + LLZTO	0.19	0.38			115
	PMC10	0.233 (50 °C)	0.32			116
	ANP-5	0.15	0.16			117
	PCL	1 (60 °C)				118
	LiPVFM	0.57				119
	ICOF-2	0.03	0.24		0.80 ± 0.02	120
	Li-con-TFSI	0.209 (70 °C)	0.34		0.61 ± 0.02	121
COF	TpPa-SO ₃ Li	0.027	0.18		0.9	122
	UiO-66-LiSS	0.06	0.21		0.9	123
	LiCON3 + 20 wt% EC	0.126 (60 °C)	0.13		0.92	124
	Im-COF-TFSI	0.029	0.32		0.62 ± 0.02	125
	PEO- <i>n</i> -UIO + 40% UIO/Li-IL	0.13	0.34		0.35	126
	dCOF-ImTFSI-60	0.097	0.28		0.72 ± 0.02	127
	$\text{CF}_3\text{-Li-Im-COF} + n\text{-BuLi} + 20\text{ wt\% PC}$	7.2	0.1		0.81	128
	$\text{CH}_3\text{-Li-Im-COF} + n\text{-BuLi} + 20\text{ wt\% PC}$	0.08	0.27		0.93	
	H-Li-ImCOF + <i>n</i> -BuLi + 20 wt% PC	5.03	0.12		0.88	
	CD-COF + LiPF ₆ + EC + DMC	2.7	0.26			129
	COF-5 + LiClO ₄	0.26	0.37			130
	LE@ACOF + EC/DEC	3.7	0.15		0.82	131
	NUS-9	12.4	0.2			132
COF-QA	NUS-10	39.6	0.21			
	COF-QA-2	211 (80 °C)	0.12			133
	COF-QA-4	200 (80 °C)	0.16			
	COF-QA-6	190 (80 °C)	0.19			
	COF-QA-EO	210 (80 °C)	0.19			

straightforward chemical reactions, potentially reducing manufacturing costs and complexity.¹³⁵ In addition, polymer materials have lower thermal stability and limited ion selectivity. Whereas, COFs can be designed to withstand higher temperatures using many approaches such as modification of chemical composition and the ion selectivity can also be tuned using various strategies such as customizing pore environments.

In summary, the activation energy of ion conduction in solid materials is a key factor that influences their efficiency and suitability for various applications. By tailoring the material properties to reduce this energy barrier, the performance of devices that rely on these materials can be significantly enhanced.

2.4 Mobile ion concentration

The ion conductivity is a measure of how easily ions can move through a medium, and it can be related to the concentration of mobile ions using the following equation:

$$\sigma = n \times q \times \mu$$

here, σ is the ion conductivity, n is the concentration of mobile ions (number of ions per unit volume), q is the charge of the ions, and μ is the mobility of the ions (how quickly an ion moves in response to an electric field).

As the concentration of mobile ions increases, the ion conductivity typically increases. This is because more charge carriers are available to carry the current. Ion mobility depends on the medium and the temperature.¹³⁶ Higher temperatures generally increase ion mobility by reducing the viscosity of the medium and allowing ions to move more freely. In solids, defects and the crystalline structure can affect ion mobility.¹³⁷ The charge of the ions affects conductivity because higher charge means more current is carried by each ion.¹³⁸ Therefore, doubly charged ions contribute more to the conductivity than singly charged ions, assuming all other factors are equal.

The mobile ion concentration and ion conductivities of various solid conductors such as inorganic and COFs are summarized in Table 1. When comparing the ion conductivities between inorganic materials and COFs, they are similar. Here, the concentrations of mobile ions in COFs are lower than those in inorganic materials. This means that the ion mobilities in COFs are faster than those in inorganic materials. This is consistent with the superior ion conducting mechanism with potentially lower energy barriers for ion conduction with COFs than inorganic materials due to their unique features.

2.5 Transference numbers

The transference number of mobile ions in the solid electrolytes is a crucial parameter that quantifies the contribution of a particular ionic species to the overall ionic current in a conductor. The measurement of transference numbers of ions can be approached using the Bruce-Vincent method with electrochemical techniques.¹³⁹ The Bruce-Vincent method involves a combination of Wagner's DC polarization test and AC impedance spectroscopy. During the DC polarization test, a symmetric two-electrode cell was used as a non-blocking setup.

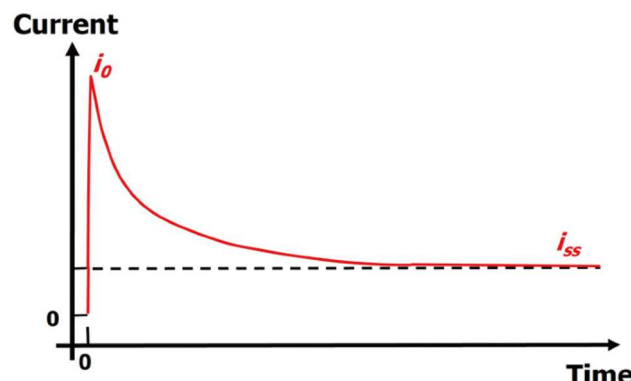


Fig. 6 Bruce-Vincent method of measuring the ion transference number from the steady state in the DC polarization curve. (Reproduced from ref. 140 under a Creative Commons CC BY license.)

Then a small step potential was applied and the resulting current over time was observed (Fig. 6).¹⁴⁰ The cell's impedances were measured before and after polarization. This process leads to the formation of a concentration gradient across the solid conductors. Before polarization of a symmetric cell, the concentrations of cationic and anionic species are almost the same on either side of the electrolyte layer. With applying a steady potential, the mobile ions (cations) move and collect on the negatively charged side, while the anions are drawn to the positively charged side. Here, both migration and diffusion push mobile cations to move in the same direction, while the anions move in the opposite direction. Therefore, the current reaches a steady state when a distinct gradient of ionic species forms across the entire electrolyte. Consequently, the transference number of mobile cations (such as lithium or sodium ions) can be calculated with the following equation:

$$t_+ = \frac{I_{ss}(\Delta V - I_0 R_0)}{I_0(\Delta V - I_{ss} R_{ss})}$$

here, t_+ is the cationic transference number, I_0 is the initial current, I_{ss} is the steady state current, ΔV is the DC polarization potential, R_0 is the initial interfacial resistance, and R_{ss} is the steady-state interfacial resistance, respectively.

The transference numbers cannot be compared between inorganic, polymer, and COFs exactly because each type of solid material can be tuned to enhance their transference numbers. For example, some inorganic solid conductors such as lithium lanthanum zirconate (LLZO) or sodium beta alumina exhibit high ion conductivities and stability. Therefore, the cationic transference numbers in these materials can be quite high. As an example, garnet-type LLZO can have high t^+ values close to unity, indicating almost exclusive cation transport.¹⁴¹ On the other hand, polymer materials generally show low transference numbers. This is because the ionic transport mechanism in polymers involves the movement of anions, and the polymer matrix may not strictly favor cation over anion mobility.¹⁴² Polymer solid conductors can suffer from significant anion mobility unless specifically designed to inhibit it. On the other hand, COFs can be engineered to have

high transference numbers by designing their pore sizes and functionalities to preferentially interact with cations, providing selective transport channels.¹⁴³ In summary, inorganic solid electrolytes tend to have high transference numbers compared to polymer materials, primarily due to their robust and rigid structures which can be highly selective for cations. COFs can also exhibit high transference numbers due to their tunability. Table 1 demonstrates the high transference numbers of inorganic and COFs compared with polymer materials. A high cationic transference number is desirable in solid electrolytes because it enhances overall efficiency, reduces detrimental side reactions, and improves the long-term stability of the energy storage and conversion devices such as batteries. Even though both inorganic and COF materials showed high transference numbers, the COFs are superior compared with inorganic materials in terms of tailorability and functionalization, flexibility, fabrication and processability, lower environmental impact, and cost effectiveness.

3. Bottom-up design strategies of ion-conductive COFs

The ion-conductive COFs can be rationally designed with bottom-up design strategies from structural control such as functionalization with ionic motifs and pore size or crystallinity regulation to incorporation of solvent or salts and processing for not only enhancing the ion conducting properties but also considering the practical feasibility (Fig. 7).

3.1 Structural control

Ion-conductive covalent organic frameworks (COFs) are advanced materials designed for specific applications, such as batteries and fuel cells, due to their ability to conduct ions. These materials can be engineered with precise structural control through pore size regulation, pore wall decoration *via* functionalization, or crystallinity regulation, to optimize their ion-conductivity.

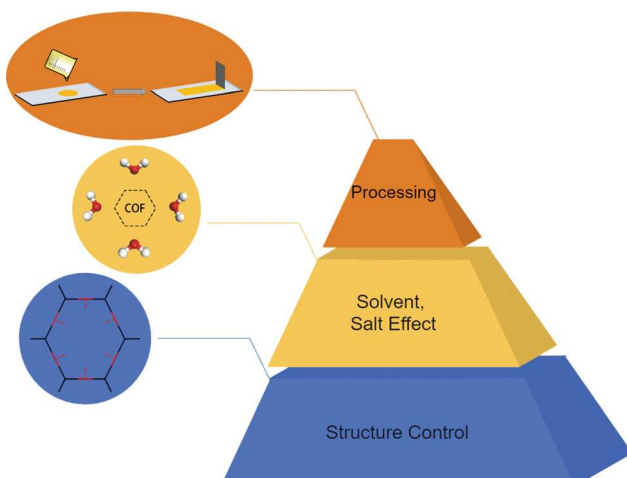


Fig. 7 Bottom-up design strategies of ion-conductive COFs.

3.1.1 Pore size regulation. The pore size of COFs is an important parameter affecting ionic conductivity. Ion conduction in COFs involves the movement of ions through well-defined nanochannels. These channels are created by the organized stacking of molecular building blocks from the COF.¹⁴⁴ The dimensions of these channels, which are directly related to the pore size, dictate how easily ions pass through.

There are mainly three roles of pore size. Firstly, larger pore sizes generally facilitate greater ion mobility. This is because bigger pores provide less resistance to ion passage, which can increase the ionic conductivity. However, while larger pore sizes can enhance conductivity by providing easier pathways for ions, they typically reduce the overall surface area when compared to smaller pores. Since surface area is crucial for ion adsorption and interaction, there is a balance to be struck between pore size and the surface area available for ionic reactions. In addition, if the pore size is too large, the interaction between the pore wall and mobile ions would be weaker, leading to low ionic conductivity. As one example which showed the relationship between the pore size and ionic conductivity of different COFs, Zhang *et al.* synthesized various COFs with different pore sizes by using different building blocks, and the COF-NUST-9 with the smaller pore size (12.4 Å) than those of COF-NUST-8 (21.2 Å) and COF-NUST-7 (20.4 Å) showed the highest ionic conductivity (Fig. 8).¹⁴⁵ This means that larger pore size does not mean high ionic conductivity due to the complex relationship between pore size and ionic conductivity of the COFs that should be considered.

There are several methods to control the pore size of COFs. The simplest method to control the pore size is through the selection of building blocks. Larger building blocks can create larger pores. For example, Zhang *et al.* synthesized similar COFs with different pore sizes by using different lengths of building blocks (Fig. 9).¹⁴⁶ The pore size distributions derived from nitrogen gas adsorption isotherms at 77 K for CN-COF-3 synthesized using longer diphenol showed a larger pore size of 18 Å than that for CN-COF-2 (11 Å). In addition, the pore size of COFs can be modulated with topological design. The topology of COFs, determined by the connectivity pattern of the building blocks, can significantly influence pore size. Designing

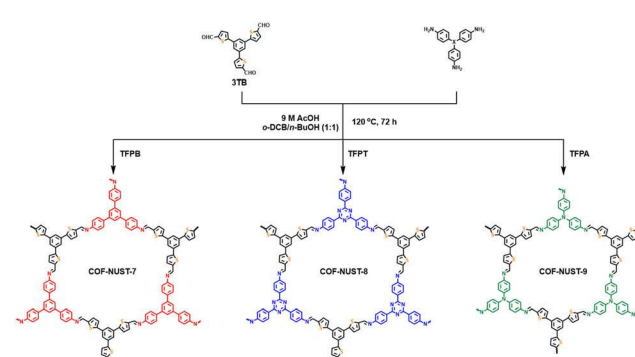


Fig. 8 Synthesis routes of COF-NUST-7, COF-NUST-8, and COF-NUST-9. (Reproduced from ref. 145 with permission from American Chemical Society.)

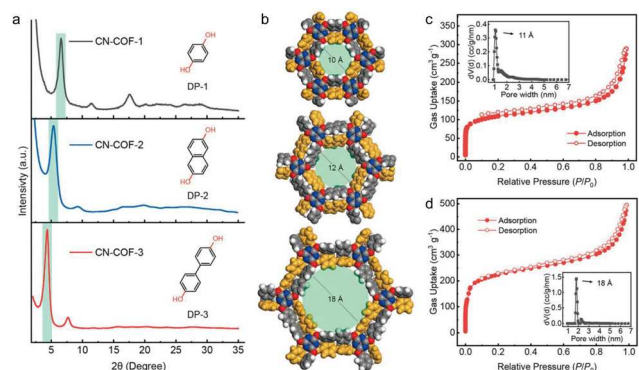


Fig. 9 Isoreticular expansion of CN-COFs. (a) Stacking of PXRD patterns showing the consistent shift of (100) peaks to smaller 2θ values and (b) AA'-stacking models of CN-COFs with the longer linkages and increasing pore sizes of 10 Å in CN-COF-1 to 12 Å CN-COF-2 and 18 Å in CN-COF-3. (c) and (d) Nitrogen adsorption and desorption isotherms recorded at 77 K and pore size distribution profiles for (c) CN-COF-2 and (d) CN-COF-3. (Reproduced from ref. 146 with permission from American Chemical Society.)

different topological networks can lead to variations in pore structures and sizes. As an example of tuning the topology to control the pore sizes in COFs, Wang *et al.* presented a strategy for introducing microporosity into COFs by partitioning the micro-pores/mesopores (Fig. 10).¹⁴⁷ This is accomplished by designing and synthesizing multicomponent COFs through imine condensation reactions involving aldehyde groups that are attached to the COF pores. Additional symmetric building blocks, like those with C_2 or C_3 symmetries, are introduced to act as agents that segment the pores, dividing them into smaller micropores. Another method to regulate pore size is optimization of the synthetic conditions such as through crystallization control. Wang *et al.* studied the crystal-size-controlled synthesis and effect of crystal size on pore size. The pore size distributions showed the disorder in nanocrystals (centered at 7.3 Å and 11.8 Å), whereas, both 1 μm - and 30 μm -sized crystals were centered at 10.9 Å.¹⁴⁸

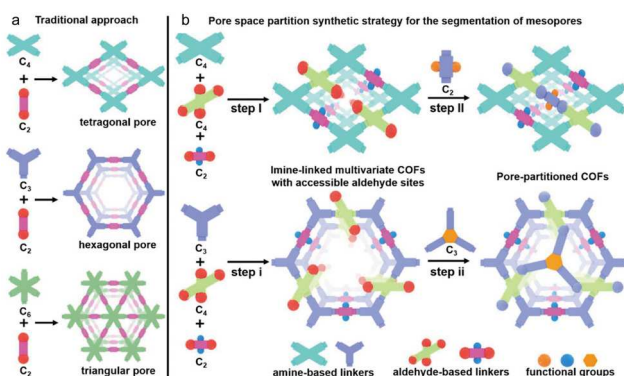


Fig. 10 (a) Schematic illustration of the traditional approach used in the synthesis of COFs. (b) Illustration of the pore partition synthetic strategy in imine-linked multivariate COFs, showing the synthesis of multicomponent COFs with predesigned accessible aldehyde sites, followed by the introduction of a symmetric building block as the pore partition agents to divide one micropore/mesopore into two or three micropores (reproduced from ref. 147 with permission from American Chemical Society).

3.1.2 Pore wall decoration by functionalization. In addition to the size, the chemical functionality within the pores can influence ionic conductivity. For example, pore walls that contain functional groups such as amine, hydroxyl, or sulfonic acid can interact with ions, potentially facilitating easier transport by stabilizing the ion within the channel.¹⁴⁹ The functional ionic groups can be divided into two types (anionic and cationic groups). As can be seen in Fig. 11, the ion conducting mechanism for different charged COFs would be different. Here, we hypothesize the mobile ions are cations such as lithium or sodium ions. For neutral COFs, there is no charged group, but polar groups. Therefore, the polar groups such as nitrogen can interact with mobile ions.¹⁵⁰ However, the interaction between polar groups and mobile ions would be weaker than the interaction between charged functional groups and mobile ions. To enhance the ionic conductivity of COFs, cationic or anionic groups can be immobilized into the pore walls. In the case of cationic COFs, the cationic groups attached in the pore wall would interact with anions (for example, the TFSI anion when using LiTFSI as a salt). Then, the free mobile cations can be more easily moved through the channels using the TFSI anion hopping site. For example, Feng *et al.* used the imidazolium-based monomers as building blocks to construct a new cationic COF (Im-COF-Br) *via* Schiff base reaction (Fig. 12).¹²⁵ Based on the ion substitution method, TFSI⁻ replaced Br⁻, which could enhance lithium-ion conductivity ($4.64 \times 10^{-4} \text{ S cm}^{-1}$ at 353 K). On the other hand, the anionic COFs can enhance the ionic conductivity by providing sites that can attract and temporarily bind cations with electrostatic interactions, aiding their transport through the channels of frameworks. For example, Lee *et al.* presented a new class of solvent-free, single lithium-ion conductors using a lithium sulfonated covalent organic framework (COF), denoted as TpPa-SO₃Li (Fig. 13).¹²² The framework, featuring well-designed ion channels, high concentrations of mobile ions, and substituted anion groups, can achieve a high ionic conductivity of $2.7 \times 10^{-5} \text{ S cm}^{-1}$ at room temperature and a lithium-ion transference number of 0.9, without the need for additional lithium salts and organic solvents. The low activation energy of 0.18 eV suggests the presence of directional ion conduction pathways within the framework.

Both methods, anionic and cationic COFs, can enhance ionic conductivity. However, cationic COFs necessarily require additional salt, whereas anionic COFs do not need extra salt as a source of mobile ions. Therefore, anionic COFs are a superior design choice for single-ion conductors.

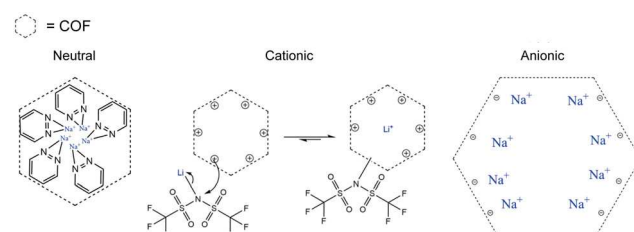


Fig. 11 Ion conducting mechanism for neutral, cationic, and anionic COFs.

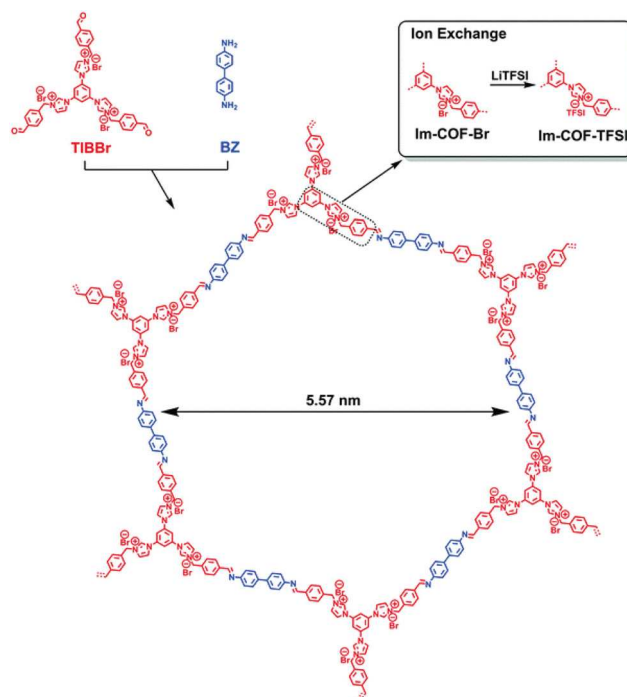


Fig. 12 Synthesis of Im-COF-Br and Im-COF-TFSI. (Reproduced from ref. 125 with permission from the Royal Society of Chemistry.)

3.1.3 Crystallinity regulation. The relationship between crystallinity and ionic conductivity of COFs involves complex interplays between structural order, porosity, and the pathways available for ion transport. In terms of pathway regularity, higher crystallinity in COFs can lead to more uniform and predictable pore sizes and shapes. This regularity can facilitate more directed pathways for ion transport, potentially increasing ionic conductivity.¹⁵¹ Regular pathways reduce the possibility of ions being trapped, thus enhancing mobility. In addition, lower crystallinity typically indicates more defects and disorder within the COF structure. While this might suggest lower ionic conductivity due to disrupted pathways, in some cases, these defects can act as additional sites for ion transport, which might enhance conductivity under certain conditions. For example, the exfoliation can lead to the production of two-dimensional COF nanosheets with the separation of a bulk crystalline material by weakening the interlayer interaction (Fig. 14).¹⁵² This reduces the overall crystallinity by disrupting the stacking of COFs. However, the remaining nanosheets may still retain significant in-plane crystallinity, preserving some of the structured pathways necessary for ionic transport. This change in crystallinity by exfoliation can affect ionic conductivity. It can increase the surface area of COFs and can expose more functional sites that can interact with ionic species. This enhanced exposure can potentially increase the ionic conductivity. In addition, the new edges created by exfoliation may have different chemical properties than the bulk material. These edges can interact with ions in a manner that either facilitates or impedes their movement, depending on the chemical nature of the edges and the type of ions. Moreover, the

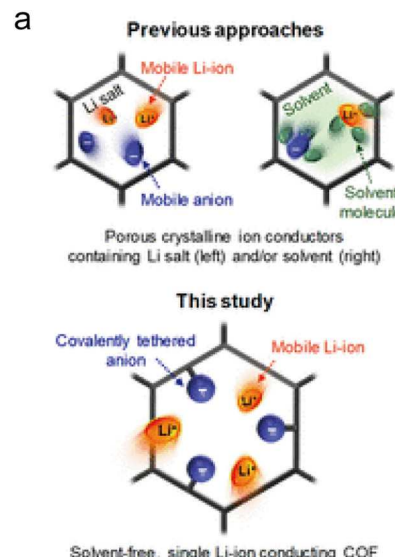


Fig. 13 (a) Conceptual illustrations of ion transport phenomena in the porous crystalline ion conductors: previous approaches (top) and this study (bottom). (b) Chemical structure of lithium sulfonated COF (TpPa-SO₃Li). (Reproduced from ref. 122 with permission from American Chemical Society.)

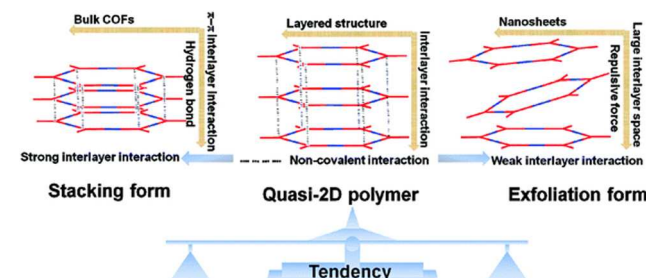


Fig. 14 Illustration of the interlayer interactions of COFs. Based on the quasi-2D polymer, the tendency towards stacking form or exfoliation form is dependent on the strong/weak interlayer interaction. (Reproduced from ref. 151 with permission from the Royal Society of Chemistry.)

thinner layers may facilitate faster ion transport across the plane of the sheets, as the distance that ions need to migrate is reduced. Furthermore, defects introduced during exfoliation can serve as active sites for ion diffusion, potentially enhancing conductivity.

There are several routes to exfoliation of COFs such as mechanical, chemical, sonication-assisted, electrochemical, thermal shock, and microwave-assisted exfoliations.^{153–159} Here, mechanical and chemical exfoliations will be mainly discussed. For mechanical exfoliation, manual peeling and ball milling can be performed. Manual peeling is the simplest form of exfoliation, often done using adhesive tape or a similar mechanism to peel off layers from bulk COF materials. A more robust mechanical approach involves using a ball mill to physically grind the COF powders under conditions that promote the delamination of layers. This can be done dry or in the presence of a solvent which can assist in the process. For example, Sun *et al.* used a ball-milling method for the exfoliation of the bulk TP-COF to create few-layer E-TP-COF (Fig. 15).¹⁵⁸ This process effectively reduced the TP-COF to a nanosheet-like structure with a thickness of approximately 2.6 nm, which is about 14 atomic layers. With the reduced thickness of the COF layers, Li-ions have a shorter and more direct path for ion conduction. On the other hand, for chemical exfoliation, chemicals can be intercalated into the layers of the COF, which expand the layers apart, weakening the interactions between them.¹⁵⁹

In addition, treatment of COFs with acids or bases can modify the edge properties or charge interactions between layers, facilitating their separation. Choosing the right exfoliation method depends on the COF's chemical stability, the desired thickness and size of the exfoliated sheets, and the specific application for which the exfoliated material is intended. It is also important to consider the scalability of the exfoliation method, especially for industrial applications.

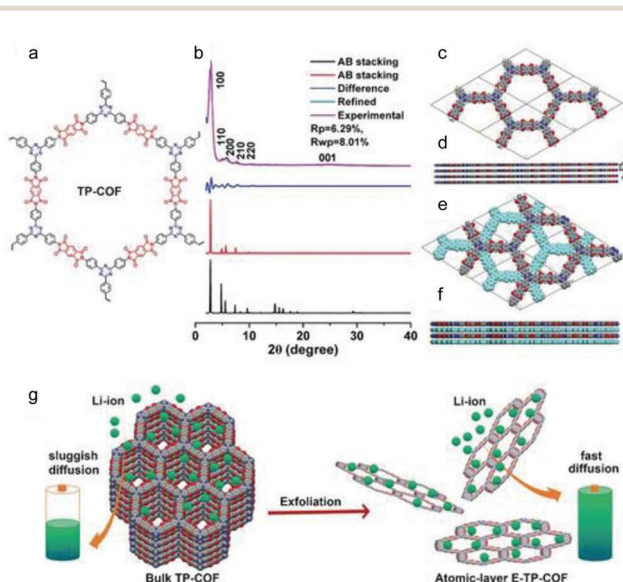


Fig. 15 (a) Chemical structure of dual-active-center modified TP-COF. (b) PXRD patterns of TP-COF with experimental, Pawley refined, difference, AA stacking, and AB stacking; calculated models for (c) and (d) AA-stacking and for (e) and (f) AB-stacking. (g) A schematic representation of the exfoliation process for TP-COF into E-TP-COF as cathodes for Li-ion batteries. (Reproduced from ref. 157 with permission from Wiley-VCH.)

3.2 Solvent and salt effect

The ionic conductivity can be enhanced by increasing the concentration of mobile ions or enhancing the mobility of ions. Here, the addition of solvent can enhance the mobility of ions, whereas the addition of salt containing mobile ions can increase the concentration of mobile ions, thereby both can boost the ionic conductivity. Table 2 summarizes the ion conducting properties of some COFs or MOFs depending on the addition of solvent or salts. It demonstrates that the COFs without additional solvent or salt showed lower ionic conductivity than the COFs with the addition of a solvent or salt.

3.2.1 Solvent effect. The addition of a solvent to COFs can significantly affect their ionic conductivity. This effect is primarily due to the interaction between the solvent molecules and the porous structure of the COFs. Solvents can be incorporated into the pores of COFs, which may change the dielectric constant of the medium within the COF.¹⁶⁰ This can enhance the dissociation of ionic species and increase the overall ionic conductivity. For example, the addition of polar solvents with high dielectric constants in COFs can improve conductivity by enhancing ion mobility through solvent-mediated interactions. As an example, propylene carbonate (PC), which is commonly used in liquid electrolytes, can be used to solvate ions in COFs to enhance the ionic conductivity.¹⁶¹ PC acts by increasing the dielectric constant of the environment around the ions, which reduces the Coulombic interaction between them, thus facilitating easier ion transport. In addition, COFs often contain various functional groups that can interact with solvents. These interactions can modify the structural environment of the COF, thereby affecting the mobility of ions. For instance, COFs with hydroxyl or amine groups might form hydrogen bonds with polar solvents, altering the framework's dynamics and potentially increasing ionic pathways.¹⁶² Moreover, the solvent can act as an additional hopping site, thereby can enhance the ionic conductivity in terms of different ion conducting pathways within one pore (Fig. 16a), from one pore to another pore by in-plane (Fig. 16b), or through-plane directions (Fig. 16c).

In summary, the impact of solvent on the ionic conductivity of COFs highlights the importance of COF design and solvent selection in developing materials for applications like batteries, sensors, and ion-exchange membranes. By investigating how different solvents influence the structure and charge transport in COFs, researchers can better design these materials for specific ionic conductivity requirements.

3.2.2 Salt effect. The addition of salts including mobile ions into the COFs can enhance the ionic conductivity by increasing the concentration of mobile ions. For example, Uribe-Romo *et al.* impregnated LiClO₄ inside the COF-5 to provide sufficient lithium-ion sources, achieving a high ionic conductivity of 2.60×10^{-4} S cm⁻¹ at room temperature.¹³⁰ Similarly, Wang *et al.* incorporated LiPF₆ inside the CD-COF, resulting in an impressive ionic conductivity of 2.70×10^{-3} S cm⁻¹ at room temperature.¹²⁹ For sodium-ion conducting COFs, Fan *et al.* utilized NaPF₆ within the NaOOC-COF, demonstrating a high ionic conductivity of 2.68×10^{-4} S cm⁻¹ at room temperature.

Table 2 Ion conducting properties summarized for COF materials depending on the addition of various solvents or salts

Solid electrolyte	Conducting ion	Additional solvent or salt	E_a eV	$\sigma_{(RT)}$ S cm $^{-1}$	Ref.
NaOOC-COF	Na-ion	Liquid electrolyte (10.0 μ L, 1.0 M) of NaPF ₆ (in propylene carbonate, PC)	0.24	2.68×10^{-4}	96
TPDBD-CNa-QSSE	Na-ion	9 wt% solvent PC with 5 wt% FEC	0.204	1.30×10^{-4}	97
MIL-121/Na	Na-ion	50 wt% 1 M NaClO ₄ in PC	0.36	1.00×10^{-4}	98
i-COF-1 (Na)	Na-ion	—	0.28	1.41×10^{-4}	Manuscript submitted
i-COF-2 (Na)	Na-ion	—	0.21	3.17×10^{-4}	
i-COF-3 (Na)	Na-ion	—	0.24	2.75×10^{-4}	
i-COF-1 (K)	K-ion	—	0.21	1.37×10^{-4}	
i-COF-2 (K)	K-ion	—	0.21	1.02×10^{-4}	
i-COF-3 (K)	K-ion	—	0.25	1.42×10^{-4}	
MOF-808-SO ₃ K	K-ion	20 μ L of anhydrous PC	0.32	3.10×10^{-5}	99
ICOF-2	Li-ion	50% PVDF, soaked in PC for 24 h	0.24	3.05×10^{-5}	120
Li-con-TFSI	Li-ion	Mixed with LiTFSI in ethanol and dried	0.34	2.09×10^{-4} (70 °C)	121
TpPa-SO ₃ Li	Li-ion		0.18	2.70×10^{-5}	122
UiO-66-LiSS	Li-ion		0.21	6.00×10^{-5}	123
LiCON3	Li-ion	20 wt% EC	0.13	1.26×10^{-4} (60 °C)	124
Im-COF-TFSI	Li-ion		0.32	2.92×10^{-5}	125
PEO- <i>n</i> -UIO	Li-ion	40% UIO/Li-IL	0.34	1.30×10^{-4}	126
dCOF-ImTFSI-60	Li-ion		0.28	9.74×10^{-5}	127
CF ₃ -Li-Im-COF	Li-ion	<i>n</i> -BuLi, 20 wt% PC	0.1	7.20×10^{-3}	128
CH ₃ -Li-Im-COF	Li-ion	<i>n</i> -BuLi, 20 wt% PC	0.27	8.00×10^{-5}	
H-Li-ImCOF	Li-ion	<i>n</i> -BuLi, 20 wt% PC	0.12	5.30×10^{-3}	
CD-COF	Li-ion	LiPF ₆ /EC/DMC	0.26	2.70×10^{-3}	129
COF-5	Li-ion	LiClO ₄	0.37	2.60×10^{-4}	130
LE@ACOF	Li-ion	EC/DEC	0.15	3.70×10^{-3}	131

However, most studies have yet to investigate the mechanisms by which these salts enhance the conductivity of COFs.⁹⁶

Salts can be introduced into the pores of COFs, where they may remain as solid particles, dissolve, or partially dissolve depending on the interaction with the framework. When salts dissolve within the pores, they dissociate into ions.¹⁶³ However, when the concentration of added salts is too high, the ionic mobility would be reduced due to higher ion aggregation and viscosity.¹⁶⁴ Therefore, the amount of salt addition should be optimized to obtain the best ionic conductivity. In addition, the dissociation energy of salts would also affect ionic conductivity. A lower dissociation energy means that the salt can more readily dissociate to produce free ions, which are essential for conductivity.¹⁶⁵ This is particularly significant in systems where the COF might not provide sufficient energy to overcome a higher dissociation barrier. The overall efficiency of ionic transport also depends on the thermodynamic compatibility between the salt and the COF material. The lattice energy of the salt and the interaction energy between the salt ions and the COF walls can influence the extent of dissociation and the mobility of the ions. The interaction energy between COF and mobile cations (E_1) should be higher than the energy between cations and anions in salts (E_2) to dissociate the salts for producing free ions to enhance the ion conductivity (Fig. 17). These energies can be modulated by incorporating ionic functional groups into the COFs that can interact with mobile ions better or the addition of salts with lower dissociation energies.

In summary, the addition of salts to COFs can dramatically improve their ionic conductivity primarily through the mechanisms of increasing the availability of free ions *via* salt dissociation and providing pathways for ion transport. The choice of salt, dictated by factors like dissociation energy and interaction

with the COF, is crucial in optimizing these materials for specific applications. On the other hand, unlike many other COFs or MOFs that exhibit high ionic conductivity typically through the addition of salts or solvents (Table 2), it is notable that the recently developed COFs (i-COF-1, 2, 3 (Na) and i-COF-1, 2, 3 (K)) by our group (Table 1) demonstrate extraordinarily high conductivity without the need for additional plasticizers or solvents. This is attributed to the strategic incorporation of sulfonate groups and directional channels within the COF structure, with the anchored sulfonate groups acting as carriers for Na or K ions. This results in salt-free, solvent-free, and uniquely efficient single Na-ion or K-ion conducting solid electrolytes.

3.3 Processing

To utilize the ionic COFs for real applications, the fabrication of freestanding COFs should be processed. There are several methods for processing freestanding COFs. Firstly, the solvent casting method can be used (Fig. 18).¹⁶⁶ This method involves dissolving both the COFs and a polymer matrix as binders in a suitable solvent, followed by casting the solution into a mold. After evaporation of the solvent, a freestanding film of COFs embedded in the polymer matrix is obtained. Its advantage is relatively simple and versatile, allowing for the incorporation of various additives to enhance mechanical strength and ionic conductivity. However, the presence of a polymer matrix can sometimes inhibit the ionic conductivity due to the insulating nature of most polymers. For example, Dichtel *et al.* reported a COF-5 film formed by evaporating the solvent from a colloidal suspension.¹⁶⁷ The size and thickness of freestanding COF films can be controlled using the solution casting method. The second method is direct synthesis of COF films. COFs can

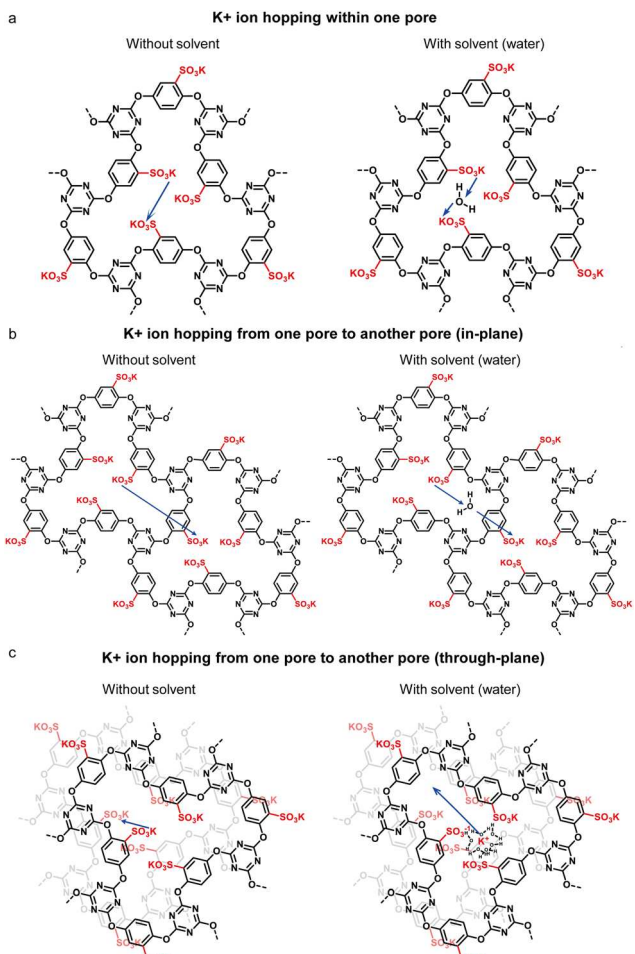


Fig. 16 Ion hopping mechanism without and with the addition of solvent (a) within one pore, (b) from one pore to another pore in the in-plane direction, and (c) in the through-plane direction.

be directly synthesized as thin films on substrates *via* chemical vapor deposition (CVD) or by using a liquid-phase epitaxy method.¹⁶⁸ This approach allows the formation of highly ordered, freestanding COF films. However, this method is technically challenging and requires precise control over synthesis conditions and is not easily scalable. Another way to make freestanding COFs is electrospinning.¹⁶⁹ It involves using an electric field to produce thin fibers from a liquid solution of COF precursors and a polymer solution. The fibers are collected as a non-woven mat that can be used as a freestanding electrolyte. It can create fibers with very high surface area-to-volume ratios, which can enhance the ionic conductivity. However, the alignment and distribution of COFs within the fibers can be inconsistent, which might affect the overall performance of the electrolyte. Forth, a layer-by-layer assembly method can be used as a technique for building freestanding COF films by alternatively depositing positively and negatively charged COF components on a substrate, allowing for precise control over film thickness and composition.¹⁷⁰ However, this method can be a slow and labor-intensive process, particularly for thicker films. Another promising method to fabricate freestanding COFs is a

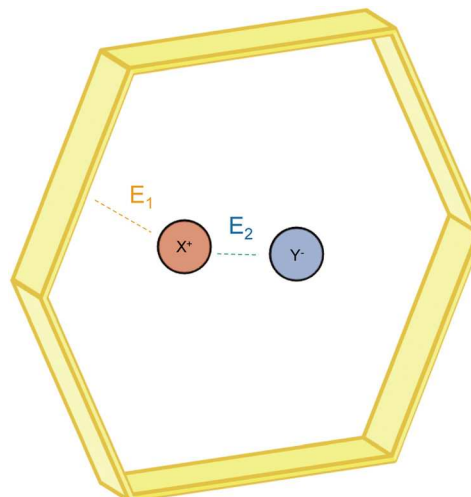


Fig. 17 Interaction energy demonstrating E_1 (energy between the COF and mobile cation) and E_2 (the energy between cation and anion in salt).

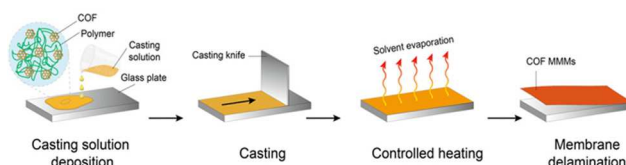


Fig. 18 Solution-casting method for making a freestanding COF. (Reproduced from ref. 165 with permission from Wiley-VCH.)

solution-processable pressing method. For example, Loh *et al.* developed hydrazone COF as a solid electrolyte and this bulk COF powder was processed in water and mechanically pressed into a freestanding pellet (Fig. 19).¹²⁴ This method is advantageous for large-scale production.

4. Applications of ionic COFs

Ionic COFs have gained attention for their applications in several fields such as energy storage, gas storage and separation, catalysis, drug delivery, sensors, and water purification and desalination. In this review, usage of COFs as solid electrolytes or membranes as ion-conducting materials for solid-state batteries and fuel cells are mainly discussed.

4.1 Solid-state batteries

Ionic COFs have shown potential as solid electrolytes in solid-state batteries due to their unique structural and chemical properties. They can be engineered to facilitate ion transport, which is crucial for the operation of batteries. Ionic COFs are characterized by a highly ordered and interconnected porous structure. This allows for the easy movement of ions through the framework. The pores can be tailored in size to optimally accommodate specific ions used in batteries, such as lithium, sodium, or magnesium ions.

One of the most studied applications of ionic COFs in solid-state batteries is as electrolytes for lithium-ion batteries.

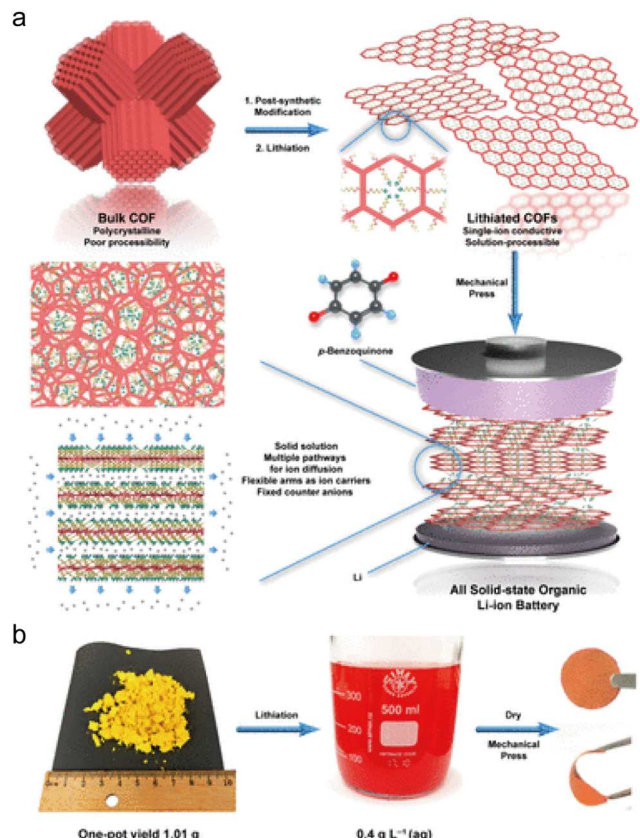


Fig. 19 COF SE for solid-state Li ion batteries. (a) Schematic illustration describing the fabrication of all-solid-state organic Li-ion batteries using lithiated COF nanosheets. (b) Gram-scale preparation of COFs for solid-state batteries. The bulk COF powder can be processed in water and mechanically pressed into a battery separator after drying. (Reproduced from ref. 124 with permission from American Chemical Society.)

For example, Wu *et al.* developed a nitrogen hybrid conjugated skeleton (NCS) based COF, consisting of triazine and piperazine rings, as a single-ion conducting solid electrolyte for solid-state lithium metal batteries (Fig. 20).¹⁷¹ This NCS-based COF solid electrolyte exhibited a high ion conductivity of 1.49 mS cm^{-1} at room temperature and a lithium transference number of 0.84 without any additional agent. The fabricated solid-state battery full cell showed stable cycling performance over 100 cycles with 82% capacity reservation at 0.5C.

Similarly, COFs can be adapted for other types of ions, such as sodium or potassium ions, which are considered as an alternative to lithium due to their abundance. For example, Fan *et al.* developed a ($-\text{COO}^-$)-modified covalent organic framework (COF) as a Na-ion quasi-solid-state electrolyte with a high sodium ion conductivity of $1.30 \times 10^{-4} \text{ S cm}^{-1}$ (Fig. 21).⁹⁶ The assembled solid-state battery full cell utilizing this COF solid electrolyte showed a stable cycling performance over 1000 cycles at 60 mA g^{-1} with a 0.0048% capacity decay per cycle and a final discharge capacity of 83.5 mA h g^{-1} .

Ionic COFs represent a promising avenue for the development of safer and more efficient solid-state batteries due to advantageous features such as flexibility, tailorability, and thermal

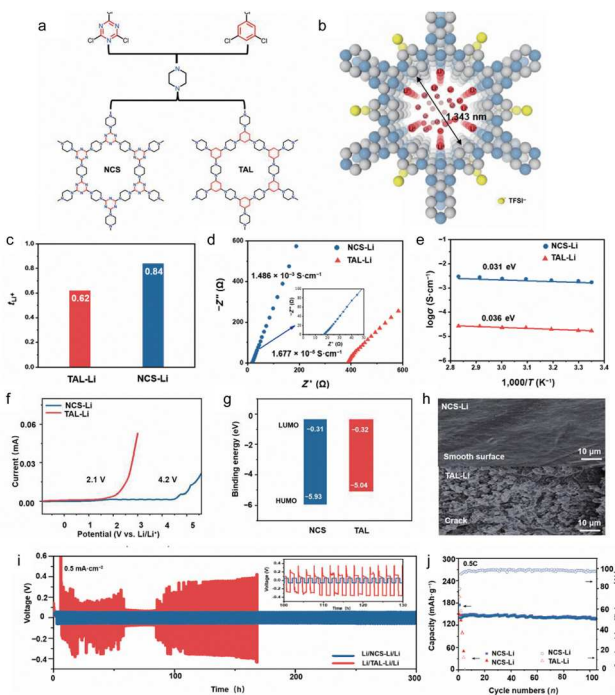


Fig. 20 (a) Synthesis of NCS and TAL. (b) The top views of the AA-stacking model of NCS-Li. (c) The ion migration number of NCS-Li and TAL-Li. (d) Impedance diagrams of NCS-Li and TAL-Li. (e) Arrhenius plot of ionic conductivity diagrams of NCS-Li and TAL-Li as a function of temperature. (f) Linear scanning curves of NCS-Li and TAL-Li. (g) HOMO and LUMO energy levels of NCS and TAL. (h) Surface structure of a cycled lithium anode in NCS-Li SSB and TAL-Li SSB. (i) Constant-current voltage profile of a lithium symmetry cell with NCS-Li and TAL-Li at 0.5 mA cm^{-2} current density. (j) Long time cycling performance of Li/NCS-Li/LiFePO₄ and Li/TAL-Li/LiFePO₄ SSBs at 0.5C. (Reproduced from ref. 171 with permission from Springer Nature.)

or chemical stability. Their ability to be custom-designed at the molecular level allows for the development of highly specialized materials tailored to specific battery technologies.

4.2 Fuel cells

For proton exchange membrane fuel cells (PEMFCs), the primary mechanism involves the movement of protons (H^+) across the electrolyte from the anode to the cathode. Ionic COFs can be designed to include proton-conductive pathways by integrating functional groups such as sulfonic acid groups, which are known for their proton conductivity. These groups facilitate proton hopping, enhancing the overall ionic conductivity of the membrane.

For example, Banerjee *et al.* synthesized a bipyridine-based COF mechanochemically and it could show an excellent proton conductivity of $1.41 \times 10^{-2} \text{ S cm}^{-1}$ (Fig. 22).¹⁷² This COF was designed to act as a solid electrolyte in proton exchange membrane (PEM) fuel cells. This COF electrolyte could inhibit the fuel crossover and maintain a stable open circuit voltage (OCV) of 0.93 V at 50 °C. As another example, Tang *et al.* utilized silk nanofibrils (SNFs) to assemble ion liquid (IL)-impregnated sulfonic acid-based conductive COFs into a stable membrane (Fig. 23).¹⁷³ The impregnated imidazole-type ILs can lower the

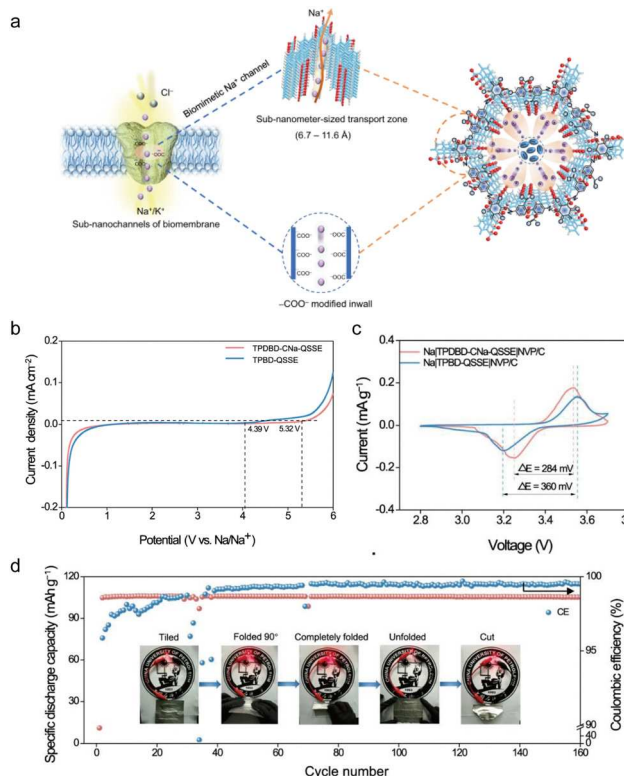


Fig. 21 (a) Biomimetic concept of sub-nanometer-sized Na^+ transport zones constructed by adjacent $-\text{COO}^-$ groups and COF inwalls (the purple and red spheres and cyan ovals denote sodium and oxygen and TFSI^- , respectively, and the cyan sticks and molecular structures denote the covalent organic framework). (b) LSV profiles of SS|TPBD-QSSE|Na and SS|TPDBD-CNa-QSSE|Na asymmetric cells. (c) CV curves of the $\text{Na}|\text{TPDBD-CNa-QSSE|NVP/C}$ and $\text{Na}|\text{TPBD-QSSE|NVP/C}$ cells at 0.1 mV s^{-1} . (d) Cycling performance of the $\text{Na}|\text{TPDBD-CNa-QSSE|NVP/C}$ tiled pouch cell at 12 mA g^{-1} for 160 cycles. The inset photos show an LED powered by the QSSE pouch cell in different states of "Tiled", "Folded 90°", "Completely folded", "Unfolded", and "Cut". (Reproduced from ref. 96 under a Creative Commons CC BY license.)

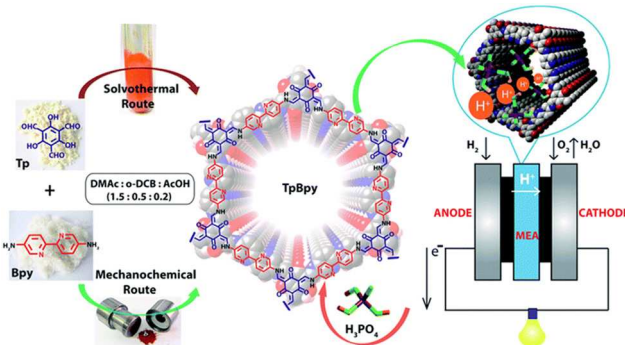


Fig. 22 Schematic representation of the synthesis of TpBpy COF [via mechanochemical (MC) as well as solvothermal (ST) routes] which upon the loading of phosphoric acid (PA) forms PA@TpBpy and is later integrated as a solid electrolyte in PEMFCs. (Reproduced from ref. 172 with permission from the Royal Society of Chemistry.)

energy barrier for proton conduction by providing more proton hopping sites. Additionally, the sulfonate groups can further



Fig. 23 Schematic illustration of preparing of the IL-COF-SO₂ H@SNF composite membrane. (Reproduced from ref. 173 with permission from Elsevier.)

reduce the energy barrier by forming strong interactions with the ILs. Therefore, this COF membrane could show a high proton conductivity of 0.224 S cm^{-1} at 90°C .

While the potential of ionic COFs in fuel cells is significant, practical application often requires extensive research and development. Issues such as scalability of synthesis, integration with current fuel cell technologies, and long-term stability and degradation need to be addressed. Advances in materials synthesis and characterization are critical to moving these materials from the laboratory to practical applications. By designing COFs specifically for ion conduction relevant to fuel cell operations, researchers can create more efficient, safer, and potentially cheaper fuel cell systems. The adaptability of COFs to various ion types and environmental conditions makes them a promising area of development in advanced energy technologies.

5. Conclusions

Ionic COFs have advantages in high ionic conductivity, thermal and chemical stability, and mechanical flexibility. They can be engineered to include functional groups that facilitate ion transport, which is crucial for high-performance solid electrolytes. In addition, they generally exhibit good stability, making them suitable for a wide range of temperatures and chemical environments. Moreover, with the right processing techniques, COFs can be made flexible, which is advantageous for wearable and portable electronic devices.

However, there are some challenges for the utilization of ionic COFs in practical devices such as scalability, cost, and uniformity/reproducibility. Many of the more precise methods for fabricating COFs are not yet scalable, limiting their commercial application. In addition, synthesis of some COFs can be costly due to the materials and conditions required, and ensuring consistent quality across larger batches of material remains a challenge. In addition, there is not enough research yet about revealing the ion conducting mechanism in terms of fundamental perspectives. Future research should be focused on not only fundamental research but also practical considerations to make COFs more commercially viable for various types of applications.

Data availability

This review article does not contain any primary data. All data discussed in this manuscript are available within the cited literature and publicly accessible sources. No new datasets were generated or analyzed during the preparation of this manuscript.

Conflicts of interest

There are no conflicts to declare.

References

- 1 A. P. Côté, A. I. Benin, N. W. Ockwig, M. O'Keeffe, A. J. Matzger and O. M. Yaghi, *Science*, 2005, **310**, 1166–1170.
- 2 X. Zhao, P. Pachfule and A. Thomas, *Chem. Soc. Rev.*, 2021, **50**, 6871–6913.
- 3 C. Li, J. Yang, P. Pachfule, S. Li, M.-Y. Ye, J. Schmidt and A. Thomas, *Nat. Commun.*, 2020, **11**, 4712.
- 4 Y. Song, Q. Sun, B. Aguila and S. Ma, *Adv. Sci.*, 2019, **6**, 1801410.
- 5 K. T. Tan, S. Ghosh, Z. Wang, F. Wen, D. Rodríguez-San-Miguel, J. Feng, N. Huang, W. Wang, F. Zamora, X. Feng, A. Thomas and D. Jiang, *Nat. Rev. Methods Primer*, 2023, **3**, 1–19.
- 6 X. Liang, Y. Tian, Y. Yuan and Y. Kim, *Adv. Mater.*, 2021, **33**, 2105647.
- 7 R. Liu, K. Tian Tan, Y. Gong, Y. Chen, Z. Li, S. Xie, T. He, Z. Lu, H. Yang and D. Jiang, *Chem. Soc. Rev.*, 2021, **50**, 120–242.
- 8 N. Huang, P. Wang and D. Jiang, *Nat. Rev. Mater.*, 2016, **1**, 1–19.
- 9 Z. Li, X. Feng, Y. Zou, Y. Zhang, H. Xia, X. Liu and Y. Mu, *Chem. Commun.*, 2014, **50**, 13825–13828.
- 10 Y. Yusran, H. Li, X. Guan, Q. Fang and S. Qiu, *EnergyChem*, 2020, **2**, 100035.
- 11 X. Liu, D. Huang, C. Lai, G. Zeng, L. Qin, H. Wang, H. Yi, B. Li, S. Liu, M. Zhang, R. Deng, Y. Fu, L. Li, W. Xue and S. Chen, *Chem. Soc. Rev.*, 2019, **48**, 5266–5302.
- 12 X. Chen, W. Sun and Y. Wang, *ChemElectroChem*, 2020, **7**, 3905–3926.
- 13 M. Li, J. Liu, T. Zhang, X. Song, W. Chen and L. Chen, *Small*, 2021, **17**, 2005073.
- 14 V. A. Kuehl, J. Yin, P. H. H. Duong, B. Mastorovich, B. Newell, K. D. Li-Oakey, B. A. Parkinson and J. O. Hoberg, *J. Am. Chem. Soc.*, 2018, **140**, 18200–18207.
- 15 N. Kaiser, S. Spannenberger, M. Schmitt, M. Cronau, Y. Kato and B. Roling, *J. Power Sources*, 2018, **396**, 175–181.
- 16 K. Kerman, A. Luntz, V. Viswanathan, Y.-M. Chiang and Z. Chen, *J. Electrochem. Soc.*, 2017, **164**, A1731.
- 17 S. Ferrari, M. Falco, A. B. Muñoz-García, M. Bonomo, S. Bruttì, M. Pavone and C. Gerbaldi, *Adv. Energy Mater.*, 2021, **11**, 2100785.
- 18 R. P. Buck, *Sens. Actuators*, 1981, **1**, 137–196.
- 19 J. B. Goodenough, *Annu. Rev. Mater. Res.*, 2003, **33**, 91–128.
- 20 Z. Gao, Q. Liu, G. Zhao, Y. Sun and H. Guo, *J. Mater. Chem. A*, 2022, **10**, 7497–7516.
- 21 G. Zhao, Z. Mei, L. Duan, Q. An, Y. Yang, C. Zhang, X. Tan and H. Guo, *Carbon Energy*, 2023, **5**, e248.
- 22 L. K. Beagle, Q. Fang, L. D. Tran, L. A. Baldwin, C. Muratore, J. Lou and N. R. Glavin, *Mater. Today*, 2021, **51**, 427–448.
- 23 Q. Xu, S. Tao, Q. Jiang and D. Jiang, *J. Am. Chem. Soc.*, 2018, **140**, 7429–7432.
- 24 H. Wang, Y. Yang, X. Yuan, W. Liang Teo, Y. Wu, L. Tang and Y. Zhao, *Mater. Today*, 2022, **53**, 106–133.
- 25 H. R. Abuzeid, A. F. M. EL-Mahdy and S.-W. Kuo, *Giant*, 2021, **6**, 100054.
- 26 H. Zhang, Y. Geng, J. Huang, Z. Wang, K. Du and H. Li, *Energy Environ. Sci.*, 2023, **16**, 889–951.
- 27 X. Li, P. Yadav and K. Ping Loh, *Chem. Soc. Rev.*, 2020, **49**, 4835–4866.
- 28 L. Frey, J. J. Jarju, L. M. Salonen and D. D. Medina, *New J. Chem.*, 2021, **45**, 14879–14907.
- 29 D. Zhu, L. B. Alemany, W. Guo and R. Verduzco, *Polym. Chem.*, 2020, **11**, 4464–4468.
- 30 Z.-B. Zhou, X.-H. Han, Q.-Y. Qi, S.-X. Gan, D.-L. Ma and X. Zhao, *J. Am. Chem. Soc.*, 2022, **144**, 1138–1143.
- 31 L. Grunenberg, G. Savasci, M. W. Terban, V. Duppel, I. Moudrakovski, M. Etter, R. E. Dinnebier, C. Ochsenfeld and B. V. Lotsch, *J. Am. Chem. Soc.*, 2021, **143**, 3430–3438.
- 32 L. Bourda, C. Krishnaraj, P. V. D. Voort and K. V. Hecke, *Mater. Adv.*, 2021, **2**, 2811–2845.
- 33 C. Qian, L. Feng, W. L. Teo, J. Liu, W. Zhou, D. Wang and Y. Zhao, *Nat. Rev. Chem.*, 2022, **6**, 881–898.
- 34 T. Xue, O. A. Syzgantseva, L. Peng, M. A. Syzgantseva, R. Li, G. Xu, D. T. Sun, R. Qiu, C. Liu, S. Zhang, T. Su, P. Su, S. Yang, J. Li and B. Han, *Chem. Mater.*, 2022, **34**, 10584–10593.
- 35 F. Haase and B. V. Lotsch, *Chem. Soc. Rev.*, 2020, **49**, 8469–8500.
- 36 L. Zhai, Y. Yao, B. Ma, Md. M. Hasan, Y. Han, L. Mi, Y. Nagao and Z. Li, *Macromol. Rapid Commun.*, 2022, **43**, 2100590.
- 37 S. Xu, H. Lin, G. Li, J. Wang, Q. Han and F. Liu, *Chem. Eng. J.*, 2022, **427**, 132009.
- 38 Y. Xie, T. Pan, Q. Lei, C. Chen, X. Dong, Y. Yuan, J. Shen, Y. Cai, C. Zhou, I. Pinnau and Y. Han, *Angew. Chem., Int. Ed.*, 2021, **60**, 22432–22440.
- 39 F. Sheng, B. Wu, X. Li, T. Xu, M. A. Shehzad, X. Wang, L. Ge, H. Wang and T. Xu, *Adv. Mater.*, 2021, **33**, 2104404.
- 40 Z. Zhang, Y. Shao, B. Lotsch, Y.-S. Hu, H. Li, J. Janek, L. F. Nazar, C.-W. Nan, J. Maier, M. Armand and L. Chen, *Energy Environ. Sci.*, 2018, **11**, 1945–1976.
- 41 Y. Choo, D. M. Halat, I. Villaluenga, K. Timachova and N. P. Balsara, *Prog. Polym. Sci.*, 2020, **103**, 101220.
- 42 J. Li, X. Jing, Q. Li, S. Li, X. Gao, X. Feng and B. Wang, *Chem. Soc. Rev.*, 2020, **49**, 3565–3604.
- 43 T. Famprakis, P. Canepa, J. A. Dawson, M. S. Islam and C. Masquelier, *Nat. Mater.*, 2019, **18**, 1278–1291.

44 Y. Wang, Y. Wu, Z. Wang, L. Chen, H. Li and F. Wu, *J. Mater. Chem. A*, 2022, **10**, 4517–4532.

45 G. Yan, S. Yu, J. F. Nonemacher, H. Tempel, H. Kungl, J. Malzbender, R.-A. Eichel and M. Krüger, *Ceram. Int.*, 2019, **45**, 14697–14703.

46 L. Buannic, B. Orayech, J.-M. López Del Amo, J. Carrasco, N. A. Katcho, F. Aguesse, W. Manalastas, W. Zhang, J. Kilner and A. Llordés, *Chem. Mater.*, 2017, **29**, 1769–1778.

47 J. Wei, H. Kim, D.-C. Lee, R. Hu, F. Wu, H. Zhao, F. M. Alamgir and G. Yushin, *J. Power Sources*, 2015, **294**, 494–500.

48 C. Wang, B. B. Xu, X. Zhang, W. Sun, J. Chen, H. Pan, M. Yan and Y. Jiang, *Small*, 2022, **18**, 2107064.

49 J. C. Bachman, S. Muy, A. Grimaud, H.-H. Chang, N. Pour, S. F. Lux, O. Paschos, F. Maglia, S. Lupart, P. Lamp, L. Giordano and Y. Shao-Horn, *Chem. Rev.*, 2016, **116**, 140–162.

50 Z. Xue, D. He and X. Xie, *J. Mater. Chem. A*, 2015, **3**, 19218–19253.

51 C. Deng, M. A. Webb, P. Bennington, D. Sharon, P. F. Nealey, S. N. Patel and J. J. de Pablo, *Macromolecules*, 2021, **54**, 2266–2276.

52 K. Zhao, H. U. Khan, R. Li, Y. Su and A. Amassian, *Adv. Funct. Mater.*, 2013, **23**, 6024–6035.

53 C. Li and G. Yu, *Small*, 2021, **17**, 2100918.

54 J. Wang, L. Liu, Y. Liu, X.-M. Zhang and J. Li, *Small*, 2023, **19**, 2207831.

55 J. Chen, P. Li, N. Zhang and S. Tang, *J. Mater. Chem. A*, 2022, **10**, 7146–7154.

56 K. Zhang, B. Zhang, M. Weng, J. Zheng, S. Li and F. Pan, *Phys. Chem. Chem. Phys.*, 2019, **21**, 9883–9888.

57 L. Zhu, H. Zhu, L. Wang, J. Lei and J. Liu, *J. Energy Chem.*, 2023, **82**, 198–218.

58 S. Ghosh, Y. Tsutsui, T. Kawaguchi, W. Matsuda, S. Nagano, K. Suzuki, H. Kaji and S. Seki, *Chem. Mater.*, 2022, **34**, 736–745.

59 Q.-W. Meng, X. Zhu, W. Xian, S. Wang, Z. Zhang, L. Zheng, Z. Dai, H. Yin, S. Ma and Q. Sun, *Proc. Natl. Acad. Sci. U. S. A.*, 2024, **121**, e2316716121.

60 S. R. Elliott, *J. Non-Cryst. Solids*, 1993, **160**, 29–41.

61 J.-F. Wu, R. Zhang, Q.-F. Fu, J.-S. Zhang, X.-Y. Zhou, P. Gao, C.-H. Xu, J. Liu and X. Guo, *Adv. Funct. Mater.*, 2021, **31**, 2008165.

62 Y. Wang, X. Liu, S. Li, T. Li, Y. Song, Z. Li, W. Zhang and J. Sun, *ACS Appl. Mater. Interfaces*, 2017, **9**, 29120–29129.

63 H. Wang, L. Sheng, G. Yasin, L. Wang, H. Xu and X. He, *Energy Storage Mater.*, 2020, **33**, 188–215.

64 H. Ma, B. Liu, B. Li, L. Zhang, Y.-G. Li, H.-Q. Tan, H.-Y. Zang and G. Zhu, *J. Am. Chem. Soc.*, 2016, **138**, 5897–5903.

65 T. Rasheed, *Sci. Total Environ.*, 2022, **833**, 155279.

66 Q. An, H. Wang, G. Zhao, S. Wang, L. Xu, H. Wang, Y. Fu and H. Guo, *Energy Environ. Mater.*, 2023, **6**, e12345.

67 H. Yang and N. Wu, *Energy Sci. Eng.*, 2022, **10**, 1643–1671.

68 X. Lan, N. Luo, Z. Li, J. Peng and H.-M. Cheng, *ACS Nano*, 2024, **18**, 9285–9310.

69 A. Mertens, I. C. Vinke, H. Tempel, H. Kungl, L. G. J. de Haart, R.-A. Eichel and J. Granwehr, *J. Electrochem. Soc.*, 2016, **163**, H521.

70 M. Guin, F. Tietz and O. Guillon, *Solid State Ion.*, 2016, **293**, 18–26.

71 F. Sun, Y. Xiang, Q. Sun, G. Zhong, M. N. Banis, Y. Liu, R. Li, R. Fu, M. Zheng, T.-K. Sham, Y. Yang, X. Sun and X. Sun, *Adv. Funct. Mater.*, 2021, **31**, 2102129.

72 Q. Ma, M. Guin, S. Naqash, C.-L. Tsai, F. Tietz and O. Guillon, *Chem. Mater.*, 2016, **28**, 4821–4828.

73 X. Wang, J. Chen, Z. Mao and D. Wang, *Chem. Eng. J.*, 2022, **427**, 130899.

74 F. Sun, Y. Xiang, Q. Sun, G. Zhong, M. N. Banis, W. Li, Y. Liu, J. Luo, R. Li, R. Fu, T.-K. Sham, Y. Yang, X. Sun and X. Sun, *ACS Appl. Mater. Interfaces*, 2021, **13**, 13132–13138.

75 A. Hayashi, K. Noi, N. Tanibata, M. Nagao and M. Tatsumisago, *J. Power Sources*, 2014, **258**, 420–423.

76 M. K. Chong, Z. Zainuddin, F. S. Omar and M. H. H. Jumali, *Ceram. Int.*, 2022, **48**, 22106–22113.

77 S. Wenzel, T. Leichtweiss, D. A. Weber, J. Sann, W. G. Zeier and J. Janek, *ACS Appl. Mater. Interfaces*, 2016, **8**, 28216–28224.

78 M. S. Whittingham and R. A. Huggins, *J. Chem. Phys.*, 1971, **54**, 414–416.

79 J. L. Briant and G. C. Farrington, *J. Solid State Chem.*, 1980, **33**, 385–390.

80 P. Hu, Y. Zhang, X. Chi, K. Kumar Rao, F. Hao, H. Dong, F. Guo, Y. Ren, L. C. Grabow and Y. Yao, *ACS Appl. Mater. Interfaces*, 2019, **11**, 9672–9678.

81 T. Won Kim, K. Ho Park, Y. Eun Choi, J. Yeon Lee and Y. Seok Jung, *J. Mater. Chem. A*, 2018, **6**, 840–844.

82 N. Wang, K. Yang, L. Zhang, X. Yan, L. Wang and B. Xu, *J. Mater. Sci.*, 2018, **53**, 1987–1994.

83 L. Zhang, K. Yang, J. Mi, L. Lu, L. Zhao, L. Wang, Y. Li and H. Zeng, *Adv. Energy Mater.*, 2015, **5**, 1501294.

84 J. W. Heo, A. Banerjee, K. H. Park, Y. S. Jung and S.-T. Hong, *Adv. Energy Mater.*, 2018, **8**, 1702716.

85 M. Duchardt, U. Ruschewitz, S. Adams, S. Dehnen and B. Roling, *Angew. Chem., Int. Ed.*, 2018, **57**, 1351–1355.

86 X. Lin, Y. Zhao, C. Wang, J. Luo, J. Fu, B. Xiao, Y. Gao, W. Li, S. Zhang, J. Xu, F. Yang, X. Hao, H. Duan, Y. Sun, J. Guo, Y. Huang and X. Sun, *Angew. Chem.*, 2024, **136**, e202314181.

87 Y. Hu, J. Fu, J. Xu, J. Luo, F. Zhao, H. Su, Y. Liu, X. Lin, W. Li, J. T. Kim, X. Hao, X. Yao, Y. Sun, J. Ma, H. Ren, M. Yang, Y. Huang and X. Sun, *Matter*, 2024, **7**, 1018–1034.

88 X. Li, Y. Xu, C. Zhao, D. Wu, L. Wang, M. Zheng, X. Han, S. Zhang, J. Yue, B. Xiao, W. Xiao, L. Wang, T. Mei, M. Gu, J. Liang and X. Sun, *Angew. Chem., Int. Ed.*, 2023, **62**, e202306433.

89 J. Zhu, Y. Wang, S. Li, J. W. Howard, J. Neuefeind, Y. Ren, H. Wang, C. Liang, W. Yang, R. Zou, C. Jin and Y. Zhao, *Inorg. Chem.*, 2016, **55**, 5993–5998.

90 Y. Sun, Y. Wang, X. Liang, Y. Xia, L. Peng, H. Jia, H. Li, L. Bai, J. Feng, H. Jiang and J. Xie, *J. Am. Chem. Soc.*, 2019, **141**, 5640–5644.

91 V. K. Singh, S. K. Singh, H. Gupta, N. Shalu, L. Balo, A. K. Tripathi, Y. L. Verma and R. K. Singh, *J. Solid State Electrochem.*, 2018, **22**, 1909–1919.

92 Q. Zhang, Y. Lu, H. Yu, G. Yang, Q. Liu, Z. Wang, L. Chen and Y.-S. Hu, *J. Electrochem. Soc.*, 2020, **167**, 070523.

93 K. M. Freitag, P. Walke, T. Nilges, H. Kirchhain, R. J. Spranger and L. van Wüllen, *J. Power Sources*, 2018, **378**, 610–617.

94 J. Ma, X. Feng, Y. Wu, Y. Wang, P. Liu, K. Shang, H. Jiang, X. Hou, D. Mitlin and H. Xiang, *J. Energy Chem.*, 2023, **77**, 290–299.

95 G. Zhao, L. Xu, J. Jiang, Z. Mei, Q. An, P. Lv, X. Yang, H. Guo and X. Sun, *Nano Energy*, 2022, **92**, 106756.

96 Y. Yan, Z. Liu, T. Wan, W. Li, Z. Qiu, C. Chi, C. Huangfu, G. Wang, B. Qi, Y. Yan, T. Wei and Z. Fan, *Nat. Commun.*, 2023, **14**, 3066.

97 R. Zettl, S. Lunghammer, B. Gadermaier, A. Boulaoued, P. Johansson, H. M. R. Wilkening and I. Hanzu, *Adv. Energy Mater.*, 2021, **11**, 2003542.

98 Y.-J. Gu, Y.-A. Lo, A.-C. Li, Y.-C. Chen, J.-H. Li, Y.-S. Wang, H.-K. Tian, W. Kaveevivitchai and C.-W. Kung, *ACS Appl. Energy Mater.*, 2022, **5**, 8573–8580.

99 J. Liang, N. Chen, X. Li, X. Li, K. R. Adair, J. Li, C. Wang, C. Yu, M. Norouzi Banis, L. Zhang, S. Zhao, S. Lu, H. Huang, R. Li, Y. Huang and X. Sun, *Chem. Mater.*, 2020, **32**, 2664–2672.

100 E. Gilardi, G. Materzanini, L. Kahle, M. Döbeli, S. Lacey, X. Cheng, N. Marzari, D. Pergolesi, A. Hintennach and T. Lippert, *ACS Appl. Energy Mater.*, 2020, **3**, 9910–9917.

101 T. Okumura, T. Takeuchi and H. Kobayashi, *ACS Appl. Energy Mater.*, 2021, **4**, 30–34.

102 G. Zhao, K. Suzuki, M. Yonemura, M. Hirayama and R. Kanno, *ACS Appl. Energy Mater.*, 2019, **2**, 6608–6615.

103 M. Weiss, D. A. Weber, A. Senyshyn, J. Janek and W. G. Zeier, *ACS Appl. Mater. Interfaces*, 2018, **10**, 10935–10944.

104 R. Schlem, S. Muy, N. Prinz, A. Banik, Y. Shao-Horn, M. Zobel and W. G. Zeier, *Adv. Energy Mater.*, 2020, **10**, 1903719.

105 T. Asano, A. Sakai, S. Ouchi, M. Sakaida, A. Miyazaki and S. Hasegawa, *Adv. Mater.*, 2018, **30**, 1803075.

106 T. Yu, J. Liang, L. Luo, L. Wang, F. Zhao, G. Xu, X. Bai, R. Yang, S. Zhao, J. Wang, J. Yu and X. Sun, *Adv. Energy Mater.*, 2021, **11**, 2101915.

107 K.-H. Park, K. Kaup, A. Assoud, Q. Zhang, X. Wu and L. F. Nazar, *ACS Energy Lett.*, 2020, **5**, 533–539.

108 Y. Kato, S. Hori, T. Saito, K. Suzuki, M. Hirayama, A. Mitsui, M. Yonemura, H. Iba and R. Kanno, *Nat. Energy*, 2016, **1**, 1–7.

109 R. Iwasaki, S. Hori, R. Kanno, T. Yajima, D. Hirai, Y. Kato and Z. Hiroi, *Chem. Mater.*, 2019, **31**, 3694–3699.

110 S. Song, S. Hori, Y. Li, K. Suzuki, N. Matsui, M. Hirayama, T. Saito, T. Kamiyama and R. Kanno, *Chem. Mater.*, 2022, **34**, 8237–8247.

111 M. Inagaki, K. Suzuki, S. Hori, K. Yoshino, N. Matsui, M. Yonemura, M. Hirayama and R. Kanno, *Chem. Mater.*, 2019, **31**, 3485–3490.

112 L. Zhou, A. Assoud, Q. Zhang, X. Wu and L. F. Nazar, *J. Am. Chem. Soc.*, 2019, **141**, 19002–19013.

113 Y. Chen, Y. Shi, Y. Liang, H. Dong, F. Hao, A. Wang, Y. Zhu, X. Cui and Y. Yao, *ACS Appl. Energy Mater.*, 2019, **2**, 1608–1615.

114 D. G. Mackanic, X. Yan, Q. Zhang, N. Matsuhisa, Z. Yu, Y. Jiang, T. Manika, J. Lopez, H. Yan, K. Liu, X. Chen, Y. Cui and Z. Bao, *Nat. Commun.*, 2019, **10**, 5384.

115 K. Khan, M. B. Hanif, H. Xin, A. Hussain, H. G. Ali, B. Fu, Z. Fang, M. Motola, Z. Xu and M. Wu, *Small*, 2024, **20**, 2305772.

116 M. Zhang, A. Yusuf and D.-Y. Wang, *J. Power Sources*, 2024, **591**, 233812.

117 D.-M. Shin, J. E. Bachman, M. K. Taylor, J. Kamcev, J. G. Park, M. E. Ziebel, E. Velasquez, N. N. Jarenwattananon, G. K. Sethi, Y. Cui and J. R. Long, *Adv. Mater.*, 2020, **32**, 1905771.

118 L. Imholt, T. S. Dörr, P. Zhang, L. Ibing, I. Cekic-Laskovic, M. Winter and G. Brunklaus, *J. Power Sources*, 2019, **409**, 148–158.

119 N. Meng, H. Zhang, S. Lianli and F. Lian, *J. Membr. Sci.*, 2020, **597**, 117768.

120 Y. Du, H. Yang, J. M. Whiteley, S. Wan, Y. Jin, S.-H. Lee and W. Zhang, *Angew. Chem., Int. Ed.*, 2016, **55**, 1737–1741.

121 H. Chen, H. Tu, C. Hu, Y. Liu, D. Dong, Y. Sun, Y. Dai, S. Wang, H. Qian, Z. Lin and L. Chen, *J. Am. Chem. Soc.*, 2018, **140**, 896–899.

122 K. Jeong, S. Park, G. Y. Jung, S. H. Kim, Y.-H. Lee, S. K. Kwak and S.-Y. Lee, *J. Am. Chem. Soc.*, 2019, **141**, 5880–5885.

123 H. Yang, B. Liu, J. Bright, S. Kasani, J. Yang, X. Zhang and N. Wu, *ACS Appl. Energy Mater.*, 2020, **3**, 4007–4013.

124 X. Li, Q. Hou, W. Huang, H.-S. Xu, X. Wang, W. Yu, R. Li, K. Zhang, L. Wang, Z. Chen, K. Xie and K. P. Loh, *ACS Energy Lett.*, 2020, **5**, 3498–3506.

125 Z. Li, Z.-W. Liu, Z.-J. Mu, C. Cao, Z. Li, T.-X. Wang, Y. Li, X. Ding, B.-H. Han and W. Feng, *Mater. Chem. Front.*, 2020, **4**, 1164–1173.

126 J.-F. Wu and X. Guo, *J. Mater. Chem. A*, 2019, **7**, 2653–2659.

127 Z. Li, Z.-W. Liu, Z. Li, T.-X. Wang, F. Zhao, X. Ding, W. Feng and B.-H. Han, *Adv. Funct. Mater.*, 2020, **30**, 1909267.

128 Y. Hu, N. Dunlap, S. Wan, S. Lu, S. Huang, I. Sellinger, M. Ortiz, Y. Jin, S. Lee and W. Zhang, *J. Am. Chem. Soc.*, 2019, **141**, 7518–7525.

129 Y. Zhang, J. Duan, D. Ma, P. Li, S. Li, H. Li, J. Zhou, X. Ma, X. Feng and B. Wang, *Angew. Chem., Int. Ed.*, 2017, **56**, 16313–16317.

130 D. A. Vazquez-Molina, G. S. Mohammad-Pour, C. Lee, M. W. Logan, X. Duan, J. K. Harper and F. J. Uribe-Romo, *J. Am. Chem. Soc.*, 2016, **138**, 9767–9770.

131 X. Li, Y. Tian, L. Shen, Z. Qu, T. Ma, F. Sun, X. Liu, C. Zhang, J. Shen, X. Li, L. Gao, S. Xiao, T. Liu, Y. Liu and Y. Lu, *Adv. Funct. Mater.*, 2021, **31**, 2009718.

132 Y. Peng, G. Xu, Z. Hu, Y. Cheng, C. Chi, D. Yuan, H. Cheng and D. Zhao, *ACS Appl. Mater. Interfaces*, 2016, **8**, 18505–18512.

133 X. He, Y. Yang, H. Wu, G. He, Z. Xu, Y. Kong, L. Cao, B. Shi, Z. Zhang, C. Tongsh, K. Jiao, K. Zhu and Z. Jiang, *Adv. Mater.*, 2020, **32**, 2001284.

134 N. Nandihalli, D. H. Gregory and T. Mori, *Adv. Sci.*, 2022, **9**, 2106052.

135 S. B. Peh, Y. Wang and D. Zhao, *ACS Sustainable Chem. Eng.*, 2019, **7**, 3647–3670.

136 J. C. May and D. H. Russell, *J. Am. Soc. Mass Spectrom.*, 2011, **22**, 1134–1145.

137 G. W. Greene, F. Ponzio, N. Iranipour, H. Zhu, A. Seeber, M. Forsyth and P. C. Howlett, *Electrochim. Acta*, 2015, **175**, 214–223.

138 C. Xu, Y. Chen, S. Shi, J. Li, F. Kang and D. Su, *Sci. Rep.*, 2015, **5**, 14120.

139 Y. Shao and C. Zhang, *J. Chem. Phys.*, 2023, **158**, 161104.

140 K. Xu, *Commun. Mater.*, 2022, **3**, 1–7.

141 Z. Zhang, L. Zhang, Y. Liu, H. Wang, C. Yu, H. Zeng, L. Wang and B. Xu, *ChemSusChem*, 2018, **11**, 3774–3782.

142 K. E. Thomas, S. E. Sloop, J. B. Kerr and J. Newman, *J. Power Sources*, 2000, **89**, 132–138.

143 D. Dong, H. Zhang, B. Zhou, Y. Sun, H. Zhang, M. Cao, J. Li, H. Zhou, H. Qian, Z. Lin and H. Chen, *Chem. Commun.*, 2019, **55**, 1458–1461.

144 L. Cao, I.-C. Chen, C. Chen, D. B. Shinde, X. Liu, Z. Li, Z. Zhou, Y. Zhang, Y. Han and Z. Lai, *J. Am. Chem. Soc.*, 2022, **144**, 12400–12409.

145 Z. Shan, M. Wu, Y. Du, B. Xu, B. He, X. Wu and G. Zhang, *Chem. Mater.*, 2021, **33**, 5058–5066.

146 Z. Lei, L. J. Wayment, J. R. Cahn, H. Chen, S. Huang, X. Wang, Y. Jin, S. Sharma and W. Zhang, *J. Am. Chem. Soc.*, 2022, **144**, 17737–17742.

147 M. Hao, Y. Xie, M. Lei, X. Liu, Z. Chen, H. Yang, G. I. N. Waterhouse, S. Ma and X. Wang, *J. Am. Chem. Soc.*, 2024, **146**, 1904–1913.

148 T. Ma, L. Wei, L. Liang, S. Yin, L. Xu, J. Niu, H. Xue, X. Wang, J. Sun, Y.-B. Zhang and W. Wang, *Nat. Commun.*, 2020, **11**, 6128.

149 H. Vardhan, A. Nafady, A. M. Al-Enizi and S. Ma, *Nanoscale*, 2019, **11**, 21679–21708.

150 C. Wang, J. Tang, Z. Chen, Y. Jin, J. Liu, H. Xu, H. Wang, X. He and Q. Zhang, *Energy Storage Mater.*, 2023, **55**, 498–516.

151 G. He, R. Zhang and Z. Jiang, *Acc. Mater. Res.*, 2021, **2**, 630–643.

152 Y. Tao, W. Ji, X. Ding and B.-H. Han, *J. Mater. Chem. A*, 2021, **9**, 7336–7365.

153 S.-X. Gan, C. Jia, Q.-Y. Qi and X. Zhao, *Chem. Sci.*, 2022, **13**, 1009–1015.

154 S. Wang, Q. Wang, P. Shao, Y. Han, X. Gao, L. Ma, S. Yuan, X. Ma, J. Zhou, X. Feng and B. Wang, *J. Am. Chem. Soc.*, 2017, **139**, 4258–4261.

155 C. Liao and S. Liu, *J. Mater. Chem. B*, 2021, **9**, 6116–6128.

156 Y. Tao, W. Ji, X. Ding and B.-H. Han, *J. Mater. Chem. A*, 2021, **9**, 7336–7365.

157 Z. Fan, K. Nomura, M. Zhu, X. Li, J. Xue, T. Majima and Y. Osakada, *Commun. Chem.*, 2019, **2**, 1–8.

158 G. Zhao, H. Li, Z. Gao, L. Xu, Z. Mei, S. Cai, T. Liu, X. Yang, H. Guo and X. Sun, *Adv. Funct. Mater.*, 2021, **31**, 2101019.

159 X. Chen, Y. Li, L. Wang, Y. Xu, A. Nie, Q. Li, F. Wu, W. Sun, X. Zhang, R. Vajtai, P. M. Ajayan, L. Chen and Y. Wang, *Adv. Mater.*, 2019, **31**, 1901640.

160 A. Zadehnazari, A. Khosropour, A. A. Altaf, S. Amirjalayer and A. Abbaspourrad, *Adv. Opt. Mater.*, 2023, **11**, 2300412.

161 L. Chen, K. Ding, K. Li, Z. Li, X. Zhang, Q. Zheng, Y.-P. Cai and Y.-Q. Lan, *EnergyChem*, 2022, **4**, 100073.

162 R.-B. Lin and B. Chen, *Chem*, 2022, **8**, 2114–2135.

163 Z.-J. Zheng, H. Ye and Z.-P. Guo, *Energy Environ. Sci.*, 2021, **14**, 1835–1853.

164 C. Geng, D. Buchholz, G.-T. Kim, D. V. Carvalho, H. Zhang, L. G. Chagas and S. Passerini, *Small Methods*, 2019, **3**, 1800208.

165 Y.-F. Huang, T. Gu, G. Rui, P. Shi, W. Fu, L. Chen, X. Liu, J. Zeng, B. Kang, Z. Yan, F. J. Stadler, L. Zhu, F. Kang and Y.-B. He, *Energy Environ. Sci.*, 2021, **14**, 6021–6029.

166 R. Wang, J. Guo, J. Xue and H. Wang, *Small Struct.*, 2021, **2**, 2100061.

167 B. J. Smith, L. R. Parent, A. C. Overholts, P. A. Beauchage, R. P. Bisbey, A. D. Chavez, N. Hwang, C. Park, A. M. Evans, N. C. Gianneschi and W. R. Dichtel, *ACS Cent. Sci.*, 2017, **3**, 58–65.

168 H. Wang, Q. Wu, H. Fu, L.-Z. Wu and X. Feng, *Chem. Commun.*, 2022, **58**, 12384–12398.

169 X. Kong, Z. Wu, M. Strømme and C. Xu, *J. Am. Chem. Soc.*, 2024, **146**, 742–751.

170 C. Wang, M. J. Park, H. Yu, H. Matsuyama, E. Drioli and H. K. Shon, *J. Membr. Sci.*, 2022, **661**, 120926.

171 Z. Cheng, L. Lu, S. Zhang, H. Liu, T. Xing, Y. Lin, H. Ren, Z. Li, L. Zhi and M. Wu, *Nano Res.*, 2023, **16**, 528–535.

172 D. Balaji Shinde, H. Barike Aiyappa, M. Bhadra, B. P. Biswal, P. Wadge, S. Kandambeth, B. Garai, T. Kundu, S. Kurungot and R. Banerjee, *J. Mater. Chem. A*, 2016, **4**, 2682–2690.

173 P. Li, J. Chen and S. Tang, *Chem. Eng. J.*, 2021, **415**, 129021.